

Heincke RV
Cruise Report HE-301

**Oceanographic and Marine Geophysical Excursion,
Bremerhaven - Helgoland**

Leg 1: 13.04.2009 - 15.04.2009

All cruise participants here

11.09.2009

Chief Scientists: *Prof. J. Bijma, Prof. V. Unnithan &
Prof. L. Thomsen*

Report compiled by Vikram Unnithan (v.unnithan@jacobs-university.de)

This is an educational excursion and forms part of the regular curriculum at Jacobs University Bremen. Students from the ESSRES PhD Research School will join in Legs I & II. *Use of data and results needs the explicit permission of the chief scientist and contributing students.*

Printed at Jacobs University Bremen,

Contents

List of Figures

List of Tables

Cruise Participants

2.1 Shipboard Scientific Party

Name	Affiliation	Contact Details
Vikram Unnithan	Jacobs University	v.unnithan@jacobs-university.de
Jelle Bijma	Jacobs University / AWI	jelle.bijma@awi.de
Albert Benthien	AWI	
Florian Neu	Jacobs university	f.neu@jacobs-university.de
Klaus-Uwe Richter		
Ulrike Richter		
Gert Rohard		
Sara Gadeberg		
Ishan Basyal	Jacobs University	i.basyal@jacobs-university.de
Maitri Fischer	Jacobs University	m.fischer@jacobs-university.de
Marta Gmez Betanzos	Jacobs University	m.gomezbetanzos@jacobs-university.de
Milen Iliev	Jacobs University	m.iliev@jacobs-university.de
Charitra Jain	Jacobs University	c.jain@jacobs-university.de
Neha Joshi	Jacobs University	n.joshi@jacobs-university.de
Gila Merschel	Jacobs University	g.merschel@jacobs-university.de
Kin Ovanesov	Jacobs University	k.ovanesov@jacobs-university.de
Katsiaryna Pabortsava	Jacobs University	k.pabortsava@jacobs-university.de
Amy Parks	Jacobs University	a.parks@jacobs-university.de
Sagar Bora	AWI	Sagar.Bora@awi.de
Christoph Hoffmann	AWI	Christoph.Hoffmann@awi.de
Christian Ihrig	AWI	Christian.Ihrig@awi.de
Franziska Kersten	AWI	Franziska.Kersten@awi.de
Jacqueline Nehring	AWI	Jacqueline.Krause-Nehring@awi.de
Ansa Lindeque	AWI	Ansa.Lindeque@awi.de
Madlene Pfeiffer	AWI	Madlene.Pfeiffer@awi.de
Theo Ridder	AWI	Theo.Ridder@awi.de
Sandra Schwegmann		
Axinja Stark	AWI	Axinja.Stark@awi.de
Ruiju Tong	AWI	Ruiju.Tong@awi.de
Heidrun Wiebe	AWI	Heidrun.Wiebe@awi.de
Nadine Wieters	AWI	Nadine.Wieters@awi.de
Mirjam Blum	ESSReS	Mirjam.Blum@awi.de
Alireza Sadeghi	ESSReS	Alireza.Sadeghi@awi.de
Michael Owonibi	ESSReS	Michael.Owonibi@awi.de
Andreas Hilboll	ESSReS	Andreas.Hilboll@awi.de
Salahaldin Juba	ESSReS	salahaldin.Juba@awi.de
Christian Stepanek	POLMAR	
Jain Ren	POLMAR	

Table 0.1:

2.2. Crew List RV HEINCKE

Name	Function
Robert Voss	Kaptain
Nils Tonnies	1 st officer
Remo Franke	2 nd officer
Jurgen Szymanski	Chief Engineer
Abu Hackman	Electrician
Horst Habecker	Cook
Dirk Gatjen	Boatswain
Gunther Lewin	Boatswain
Jose marujo	AB
Bernhard Pruchnow	SM
Kurt Siefert	AB
Bruno Amaral	AB

Table 0.2:

1 Objectives

by Jelle Bijma & Vikram Unnithan

1.1 Education

1.2 Scientific Research

2 Cruise Narrative

by Maitri Fischer

Important - All times are UTC time (Local time -2h).

Day1 - April, 13th 2009

Time	Event	Location (Degrees)	Equipment
5:00 Pre 8:00	Echosounder turned on Arrival of all participants. Jacobs students, AWI students, ERASMUS students and instructors. Loading of equipment and food stuff.	Bremerhafen Port Bremerhafen Port	
8:00	the RV Heincke left port, heading for first destination	Bremerhafen Port	
9:00	Jacobs Undergraduate student tasks handed out at random.		
12:47	Arrive at Way pt. 1. Beginning of line (BoL) for Multibeam.	lon=7.758, lat= 53.998	Multibeam
13:12	Arrive at way pt2. End of line (EoL) for Multibeam.	lon =7.758, lat=54.048	Multibeam
13:17	BoL for the multibeam.	lon =7.758, lat=54.048	Multibeam
13:40	Arrive at way pt 3. EoL for the multibeam.	lon =7.757, lat=53.997	Multibeam
13:57	Deployment of CTD	Way pt 3	CTD
14:20	Deployment of Micro Sediment Corer	Way pt 3	Micro Sediment Corer
14:25	leave to way pt 4	Way pt. 3	
15:04	BoL for the multibeam.	lon =7.783, lat=54.042	Multibeam
15:08	Beginning of magnetics reading. Milen Iliev, Vikram Unnithan and a driver on a small rubber boat towed the magnetometer.	lon= 7.782, lat=54.04	Magnetometer
15:11	The sidescan was deployed and BoL for the sidescan.	lon= 7.013, lat= 54.001	Sidescan sonar
16:34	EoL for the multibeam.	lon =8.064, lat=54.068	Multibeam
16:51	EoL for the Sidescan	lon= 8.002, lat= 54.001	Sidescan Sonar
16:52	Way pt 5 reached and EoL for magnetics measurement.	lon=8.115, lat=54.073	Magnetometer
17:11	BoL for Multibeam.	lon=8.084, lat=54.070	Multibeam
18: 55	EoL for Multibeam, and RV Heincke docked in Helgoland.	lon=7.894, lat=54.173	Multibeam

Table 2.1: Day 1, 13.April.2009

Day2 - April, 14th 2009

Time	Event	Location (Degrees)	Equipment
5:00	Echosounder turned on	Helgoland port	Echosounder
6:05	RV Heincked left port Helgoland heading to Way pt 1.		
6:11	BoL for the Multibeam (just some small runs before the first way pt is reached)	lon=7.898 lat=54.176	Multibeam
6:29	Sidescan was started (BoL)	lon= 7.015, lat=54.002	Sidescan
6:27	EoL for Multibeam and BoL for Multibeam Profile 9.	lon=7.893, lat=54.141	Multibeam
6:33	Way point 1 was reached. Stop of Multibeam profile 9 (EoL). BoL for new Multibeam, profile 10.	lon= 8.065, lat=54.267	Multibeam
6:49	Arrive at Way pt 2. End of Sidescan line (EoL) and multibeam, and BoL for Multibeam (profile 11).	lon=7.014 , lat=54.003	Sidescan, Multibeam
7:04	Arrive at Way pt 3. CTD deployed and EoL for Multibeam.	lon=7.836 , lat=54.154	CTD, Multibeam
7:20	Deployment of Plankton Multinet.	Way pt 3	Plankton Multinet
7:33	Arrive at Way pt 4. BoL for Multibeam, profile 13. BoL for Sidescan (line 3).	lon=7.014 , lat=54.002	Multibeam, Sidescan
8:17	EoL for Sidescan (line 3) and EoL for Multibeam	lon=7.739° , lat=54.151°	Sidescan
8:18	BoL for Sidescan (line 4)	lon=7.012 , lat=54.003	Sidescan
8:22	Arrive at Way pt 5. BoL for Multibeam (profile 14)	lon=7.738 , lat=54.150	Multibeam
8:34	Arrive at way pt 6. EoL for sidescan and Multibeam.	lon=7.7390 , lat=54.132	Sidescan, Multibeam
09:46	EoL for Multibeam (line 15) and BoL for Multibeam line 16.	lon= 7.739, lat=54.132	Multibeam
09:47	BoL number 2 of magnetics.	lon= 7.737, lat=54.132	Magnetometer
10:57	EoL 2 of magnetics and Multibeam.	lon= 7.957, lat=54.133	Magnetometer, Multibeam
11:15	Arrive at Way pt 9. BoL for multibeam.	lon=7.964, lat= 54.131	Multibeam
12:52	Arrive at Way pt 10. EoL for Multibeam (line 17) and EoL for Sidescan.	lon= 7.961, lat=54.245	Multibeam

Table 2.2: Day 2, 14.April.2009

12:53	BoL for Sidescan and BoL for Multibeam	lon= 7.961 lat= 54.245	Sidescan and multi-beam
12:59	EoL for sidescan and BoL for sidescan. EoL for Multibeam, and BoL for multibeam line 19.	lon= 7.963, lat=54.245	Multibeam, Sidescan
13:34	EoL for sidescan and multi-beam.	lon= 895, lat=54.245	multibeam, Sidescan
13:35	Arrive at way pt 10. Beginning of grid manover for multibeam and sidescan. Refer to Profile number 20 - 25 from Multibeam measurements table and line 12-22 for Sidescan in the sidescan measurements table.	lon=7.876, lat= 54.247	Multibeam, Sidescan
14:40	End of Grid manover for multibeam and sidescan.	lon=7.885, lat=54.258	Multibeam, Sidescan
14:40	BoL for multibeam (profile 26)	lon=7.885, lat=54.258	Multibeam
15:03	EoL for multibeam	lon=7.820, lat= 54.248	Multibeam
15:04	BoL for multibeam (profile 27)	lon=7.818, lat=54.247	Multibeam
15:10	EoL for multibeam	lon=7.800, lat= 54.258	Multibeam
15:11	BoL for multibeam (profile 28)	lon=7.799, lat= 54.245	Multibeam
15:15	Deployment of CTD	lon=7.798, lat=54.245	CTD
15:25	Sediment boxcore deployed	lon=7.798, lat=54.245	Boxcore
16:05	EoL for multibeam profile 28	lon=7.898, lat=554.171	Multibeam
16:15	RV Heincke Docked in Helgoland.	Port Helgoland	

Table 2.3: Continuation of table 2.2

Main Equipment on Board

- CTD
- sediment boxcore
- sediment microcore
- plankton multinet
- magnetometer
- sidescan sonar
- multibeam
- navigation hardware
- Simrad Echo-sounder
- Fisheries Echo-sounder

Some Pictures of the Equipment



Figure 2.1: Boxcore

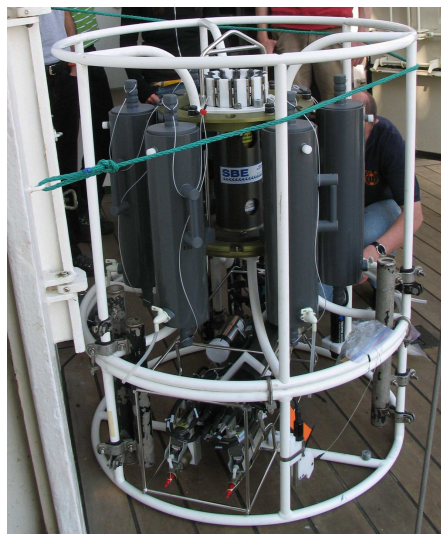


Figure 2.2: CTD



Figure 2.3: Side Scan Sonar



Figure 2.4: Magnetometer



Figure 2.5: Plankton Multinet



Figure 2.6: Sediment Micro-core

3 Navigation

3.0.1 DESCRIPTION OF INSTRUMENTS

As the navigation team on board, we were mostly involved with keeping a record of the path of the vessel during the cruise. The Differential Global Positioning System (DGPS) was the main navigation system used on the Heinke research vessel. In this section we analyse the theory of GPS, DGPS and GarMin.

- **Global Positioning System (GPS)**
GPS is a global navigation satellite system. It uses a constellation of between 24 and 32 medium Earth orbit satellites that transmit precise radiowave signals, which allow GPS receivers to determine the current location, time, and the velocity of a certain body on Earth. GPS is widely used for navigation, map-making, land surveying, commerce, scientific use, tracking, surveillance, etc. The work of a GPS device is based on receiver that calculates its position by precisely timing the signals sent by the GPS satellites high above the Earth. Each satellite continually transmits messages containing the time the message was sent, precise orbital information, and the general system health and rough orbits of all GPS satellites. The receiver measures the transmit time of each message and computes the distance to each satellites to determine the receiver's location. The position is displayed, perhaps with a moving map display or latitude and longitude; elevation information may be included (for example, on the OLEX operating system, if was possible to switch on and off the elevation indicator). Many GPS units also show derived information such as direction and speed, calculated from position changes.([?]). On board the Heinke, we used one GPS terminal that transferred information of position and time to different softwares. This enabled the precise tracking of the ship at every point of time.
- **Differential Global Positioning System (DGPS)**
DGPS is an enhancement to GPS that uses a network of fixed, ground based reference stations to broadcast the difference between the positions indicated by the satellite systems and the known fixed positions. DGPS is used on ships, as was used on the Heinke. Its operation is based

on a reference station that calculates differential corrections for its own location and time. Users may be up to 200 nautical miles from the station, however, some of the compensated errors vary with space: specifically, satellite ephemeris errors and those introduced by ionospheric distortions. For this reason, the accuracy of the DGPS decreases with distance from the reference station. ([?])

- **GarMin**

GarMin is named after inventors Gary Burnell and Min Kao. Garmin is another GPS hand-held device that is used, for instance, when Magnetometry measurements are conducted. All current GarMin devices can display the current location on a map. The maps are vector based and stored in the built in memory or loaded additional flash media. The built in, so called 'basemap', displays all country borders and major cities. On the Heincke, GarMin was used on the dinghy send out for Magnetometry. This enabled us to get the precise position of the magnetometer as the dinghy trailed behind the vessel by about 200m. ([?])

3.0.2 METHODS OF DATA COLLECTION

As discussed in the previous section, data was obtained on the Heincke though DGPS. This data is received on softwares in the form of NMEA strings sent to the data acquisition systems on board. In this section, we discuss the methods of data collection by the DGPS.

- **National Marine Electronic Association Strings (NMEA Strings)**

NMEA is a combined electrical and data specification for communication between marine electronic devices. GPS receiver communication is defined within this specification. Most computer programs that provide real time position information understand and expect data to be in NMEA format. This data includes the complete PVT (position, velocity, time) solution computed by the GPS receiver. The idea of NMEA is to send a line of data called sentence or string that is totally self contained and independent from other sentences (strings). There are standard strings for each device category and there is also the ability to define proprietary sentences from use by individual company. All of the standard sentences have two letter prefix that defines the device that uses that sentence type. For GPS receivers the prefix is GP, which followed by a three letter sequence that defines the sentence content. ([?]) There are many sentences in the NMEA standard for all kinds of devices that may be used in the Marine environment. Some of the ones that have applicability to GPS receivers are listed

below as an example:([?])

GGA: time position, and fix data type.

GLL: latitude, longitude, UTC time of position fix and status.

GSA: GPS receiver operating mode, satellites used in the position solution, and DOP values.

GSV: The number of GPS satellites in view satellite, ID numbers, elevation, azimuth, and SNR values.

MSS: Signal-to-noise ratio, signal strength, frequency, and bit rate from a radio-beacon receiver.

RMC: Time, date, position, course and speed data.

VTG: Course and speed information relative to the ground.

ZDA PPS timing message (synchronized to PPS).

- Data Acquisition and Distribution (DATADIS)

DATADIS was the data acquisition system on board the Heincke. It is a software designed for continuous recording of nautical, meteorological, survey, fishery and ship's data and their digital and/or graphical processing, recording and storage. Data is stored as a daily file for at least 4 weeks in addition on the SYSTEM-PS and can be used by the SYSTEM-PS and via Ethernet LAN (e.g. Challenger was used on board the Heincke to store and acquire data by all scientists on board. The same server is now accessible with the detailed records of all experiments conducted and navigation data.) by any USER-PC for longterm graphic displays and individual Voyage Recorder. All display, print and storage formats can be created or changed by the client without any programming knowledge, using 'Drag and Drop' method.([?])

3.0.3 DATA PROCESSING TECHNIQUES

As describes above, data is obtained onto the system in the form of NMEA strings from the GPS or to the data acquisition system of Heincke DATADIS. The processing of data for the Navigation team involves making the data readable by different softwares. The necessary columns of data, such as the coordinates, windstrength etc from the NMEA strings, for example, are separated into different files such that they can be used differently by different software

such as ArcGIS or GMT. The processed data is then used on board on the OLEX system to keep a continuous track of the vessel's movements. At any point of time, the ships velocity, water depth, direction, windspeed etc can be determined with this data.

The Navigation team focusses mostly on the navigation coordinates, i.e latitude and longitude data but keeps a record of all other data obtained on thr GPS since it is required by the scientists conducting the other experiments. Coordinates are obtained on the GPS in the digree- minute format and need to be first converted into the readable decimal-degree format. This is done using the comand "awk" in the UNIX terminal. For example, the command-

```
awk '{print int($1/100)+(($1-100*int($1/100))/60),int($2/100)+(($2-100*int($1/100))/60)}' file1.tex > file2.tex
```

will convert the necessary coloumns into the decimal-degree format and transfer the data from file1 to file2. This processed data can now, for example, be used by us in plotting the events on the cruise on a map. The experiments conducted on board are broadly divided into two categories- point experiments, conducted while the vessel was stationery and track experiments, conducted along a certain curise track. For each kind of experiment, the navigation teams keep a record of the coordinates of the location of the vessel at the begin and the end of the experiment and the exact time the experiment was conducted at. The following section has the required detailed plots, plotted on GMT.

3.0.4 RESULTS AND ANALYSIS

Using the techniques described above we created detailed plots and maps of all the scientific experiments conducted on Heincke. With each experiment, details such as the time, coordinates, depth, windstrength and speed were recorded by the DGPS. The navigation softwares on board were constantly updated by the received data as the ship moved. The following maps were made using GMT (Generic Mapping Tools: a software for the plotting and manipulation of cartesian data sets) and ArcGIS (An ESRI developed Geographic Information System). Different plots were created for different measurements to ensure the clarity of activities conducted on board. The caption on each map describes the method being recorded. In the section after that, we discuss the shortcomings of GPS and the possible errors in the data plotted.

Figure 3.1: General Map of the Heinke cruise, 13-15 April 2009. The map shows the route taken from Bremerhaven in North-West Germany to the island of Helgoland. Bathymetry data is included in the background since this data was used in addition to maps of the seafloor to determine the Way Points in the route of the cruise. Regions with varying bathymetry were chosen and the vessel was made to move over regions where known shipwrecks were lying. Often during the cruise, the course of the vessel had to be altered to suit the experiments being conducted.

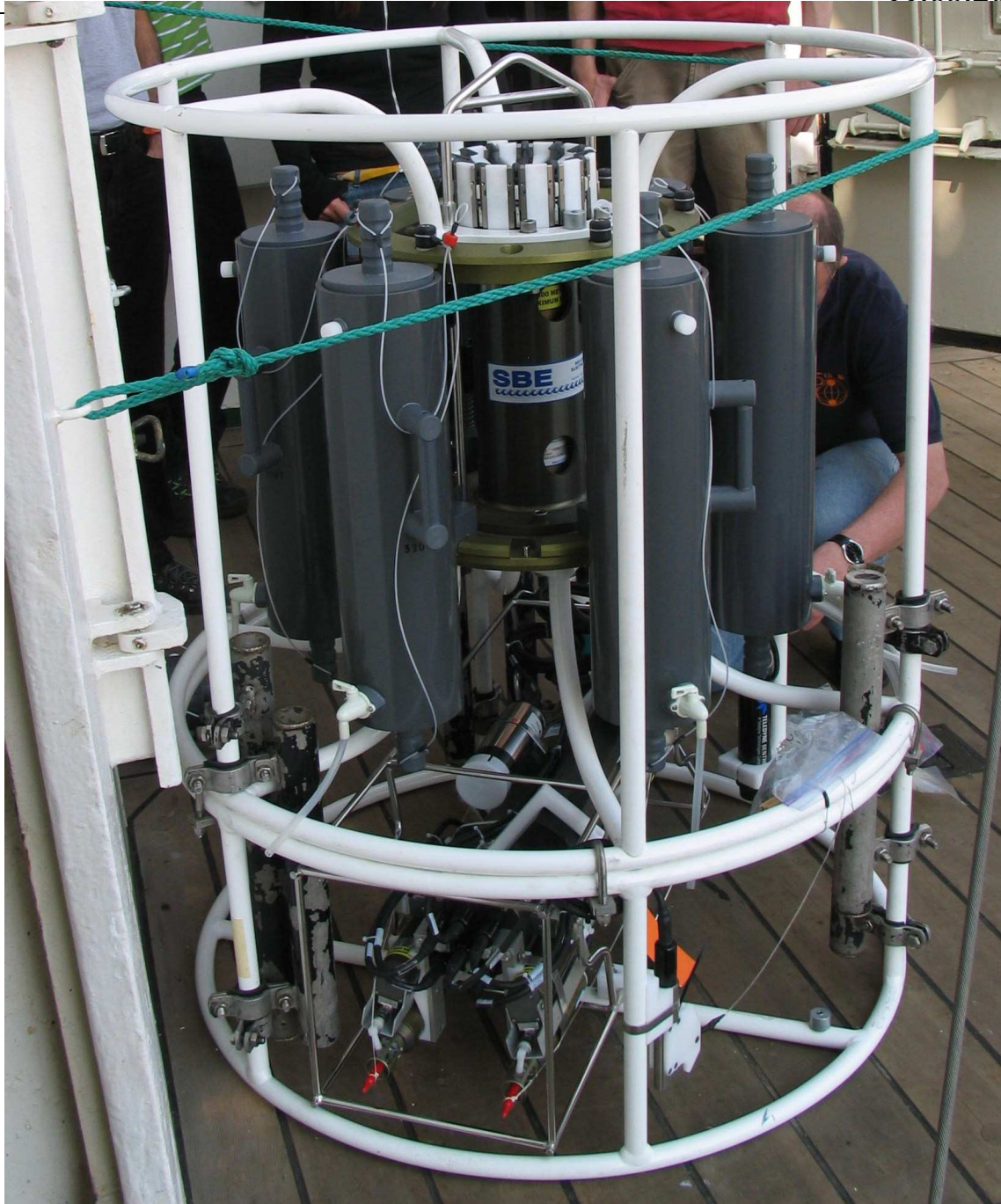


Figure 3.2: CTD measurements were made when the vessel was stationary. The CTD was released into the water at three points during the cruise to make conductivity, depth and temperature measurements. The points and times of the CTD are located on this map.

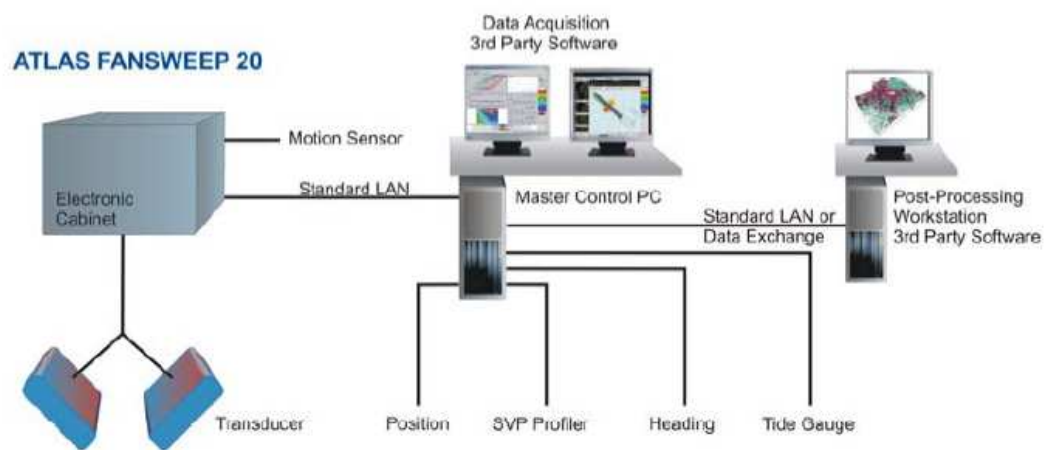


Fig. Typical ATLAS FANSWEEP 20 System Configuration

Figure 3.3: Multibeam measurements were made on board for certain sections on the cruise track. These sections are marked on the map with the start and end time for each section being indicated. The choice of the cruise course reflects the locations of known shipwrecks and other bathymetric variances.

Figure 3.4: Side-scan measurements were made by the sidescan instrument that was released into the water and towed behind the ship at a certain distance. Care needed to be taken that a certain speed on the ship was maintained such that the sidescane does not trail along the seabed. Also, notice the loops made on the path of the vessel before the end of the measurements. This is done on purpose so as to prevent the tangling of the sidescan instrument wires while the ship changed direction (and to prevent interference with the Magnetometry recordings) and to maintain the speed of the vessel.

We note a few significant points from the data plotted above, such that the accuracy of the cruise track may not be entirely correct sometimes, since many measurements are plotted to be at a slight distance from the determined cruise track. Also, the vessel's GPS records different coordinates of location during the time when the vessel is assumed to be stationary. This error could be result of the movement of the vessel by the waves in the ocean, but at certain points, the error is significantly large such that corrections in the recorded coordinates needed to be made before plotting the maps. Though the coordinates provide a reliable output when represented on the map, it is important to discuss the error sources of GPS, as done in the proceeding section.

3.0.5 DISCUSSION OF LOGGED DATA AND CONCLUSIONS

From the Results and Analysis section we notice that the data measured by the DGPS on board the Heincke is very precise, but has errors arising due to its inaccuracy at certain places. The coordinates recorded were good indicators of the vessels location on the map but the errors are more easily noticeable when different coordinate points were recorded during the time the vessel was assumed to be stationary. Also, some of the recorded coordinates for the experiments were completely off the cruise track and had to be corrected manually to set them to the right locations. In this section we analyse the reasons for these errors and assess whether the final data obtained is reliable for the navigation team or not.

Some of the possible errors of GPS include selective availability which means that, first, civil GPS receivers position determination is less accurate and fluctuates about 50 meters error. This problem however is slightly rectified because Heincke uses DGPS, but the errors in the locations are still noticeable. Also, to indicate correct satellite geometry certain DOP values in the NMEA sentence

\$GPGSA

have to be larger than 5. NMEA strings without accurate DOP values amplify other inaccuracies in the coordinate data received. Atmosphere effects cause reduction in the speed of propagation of radiowaves received from the satellites in the troposphere and ionosphere. The velocities are slower in these regions. Civil receivers are usually not capable of correcting these unforeseen runtime changes which are also sometimes caused by strong solar winds.

Other common inaccuracies include rounding errors and calculation errors of the receiver up to approximately 1m. Relativistic effects require GPS navigation to be accurate to 20-30 nanoseconds. Therefore, fast moving satellites and receivers have to be adjusted accordingly. Having discussed these general error

sources, we notice other errors in the readings that might arise due to fact that the GPS receiver of the ship marks its position at the exact center of the ship. Some experiments were carried out off the deck of the ship at a slight distance, thus causing errors in recorded coordinates ([?]).

Despite these errors, we notice that the results we obtained are very reliable. Some of us were actually fascinated by how accurate and precise all the readings were and the amount of data carried in each NMEA string. The results can be successfully reused for future excursions and by the students of 2011, Jacobs University during their Data Analysis classes on the Heincke Excursion 2009.

Figure 3.5: The other instruments used on board were the Minicorer (MIC), Multiple Net (MN) and Small Grab Box(SBG), all indicated on this map. The Messfahrt points show the points where the dinghy left the vessel for the Magnetometry measurements. The coordinates of the dinghy were recorded separately by the people on the dinghy using GarMin as described before.

Bibliography

- [1] http://www.en.wikipedia.org/wiki/Global_Positioning_System,
Global Positioning System
- [2] http://www.en.wikipedia.org/wiki/Differential_GPS, Differential
Global Positioning System
- [3] <http://www.en.wikipedia.org/wiki/Garmin>, GarMin
- [4] <http://www.gpsinformation.org/dale/nmea.htm>, NMEA Data
- [5] <http://www.sparkfun.com/datasheets/GPS/NMEA%20Reference%20Manual1.pdf>,
NMEA Reference Manual
- [6] http://www.maritech-engineering.de/html/datadis_engl.html,
Maritech Engineering, DATADIS
- [7] <http://www.kowoma.de/en/gps/errors.htm>, GPS explained: Error
Sources

4 Multibeam

by Amy Parks, Charitra Jain, Gila Merschel

4.1 Aims

4.1.1 Instrument used, general principals of multibeam

The ATLAS FANSWEEP 20/100 is a wide swath 100 kHz multi-beam echosounder designed for survey of coastal areas to depths of 600 m. It has a dual head transducer that provides swath coverage of 6 times the water depth for bathymetry and up to 12 times the water depth for side scan imagery. It combines the advantages of beamforming and interferometric phase measurement techniques to the benefit of a large coverage together with high accurate depth measurements.

TRANSDUCER CONFIGURATION A pair of identical hydroacoustic transducers is installed in the hull of the ship in V-shape. Each transducer consists of 26 rows of elements arranged in two transmission sections and 10 reception sections. Each section provides an inner beam (wide beam) and an outer beam (narrow beam). Generally, all four beams are active but under extremely noisy conditions (air bubbles or mud in the water column) the outer beams are switched off in order to reduce the amount of erroneous echoes with high amplitudes.

Due to the specific form and arrangement of the beams, sound is directed from either side of the ship into the entire half-space from almost the horizontal to the vertical. In all 4 beams, very short transmission pulses with the appropriate frequency are transmitted at the same time. If, for example, it is assumed that the water bottom is flat and horizontal, the transmission pulses with the higher frequency hit the bottom first (a). Parts of the bottom lying further away in the transverse direction are reached later by the transmission pulse (b). The lower-frequency transmission pulses cover that part of the bottom that lies further away in the transverse direction (c).

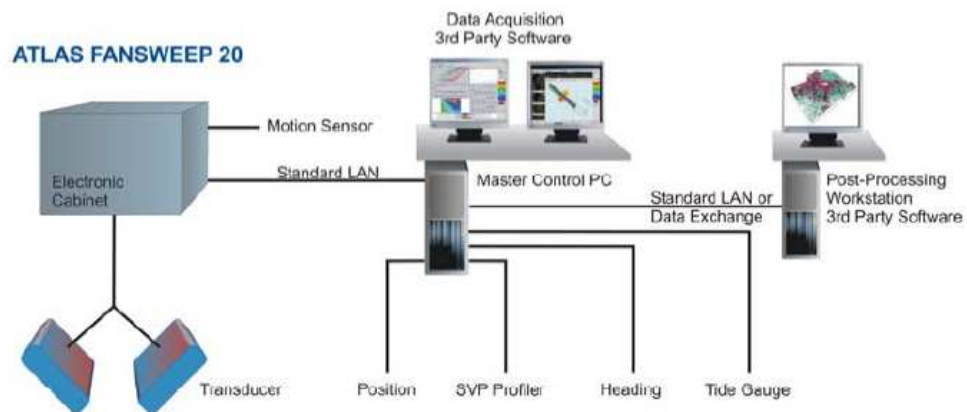


Fig. Typical ATLAS FANSWEEP 20 System Configuration

Figure 4.1: Setup of the instrument[?]

FANSWEEP 20 - Standard Configuration

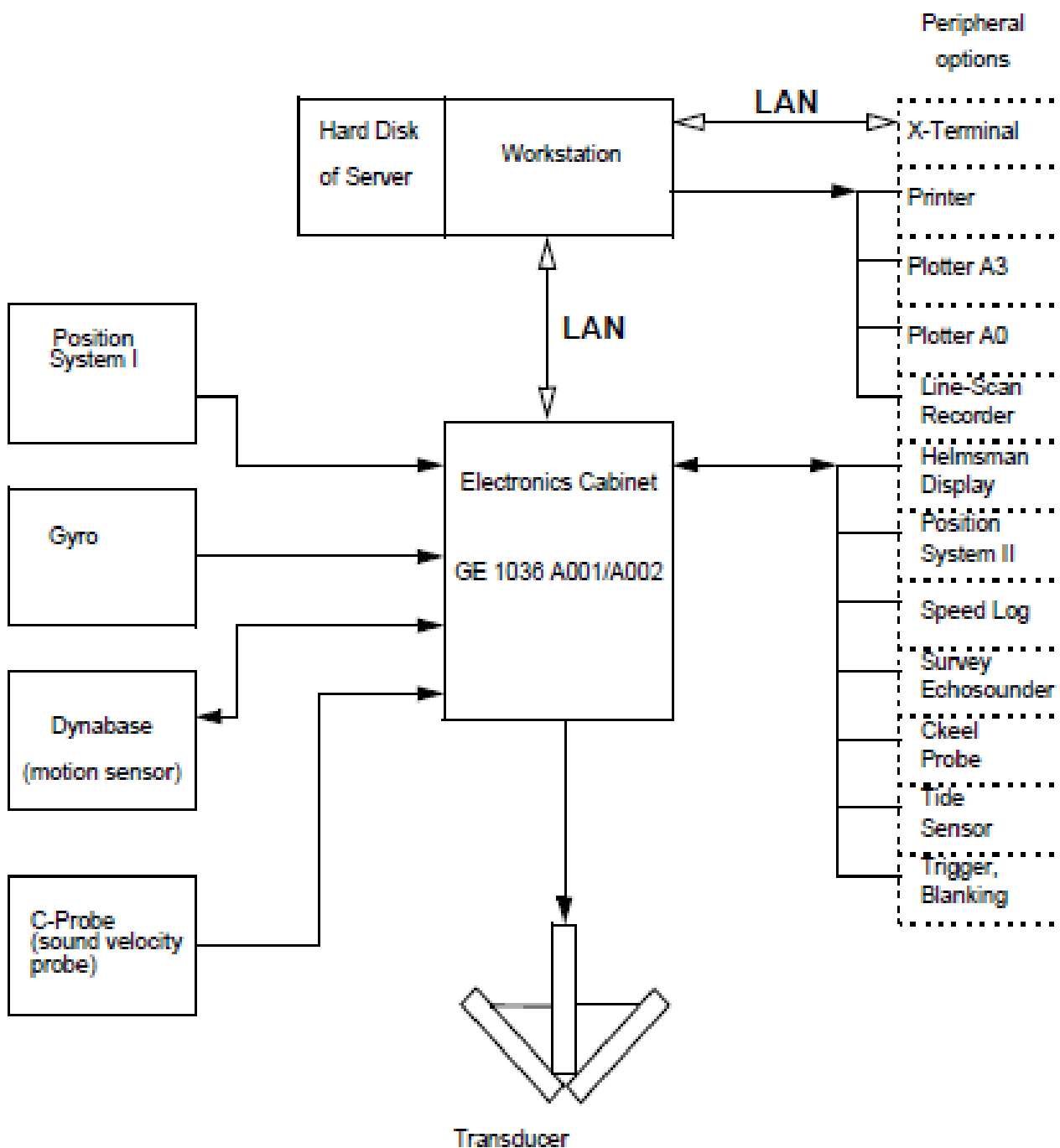


Figure 4.2: Flow diagram of the instrument[?]

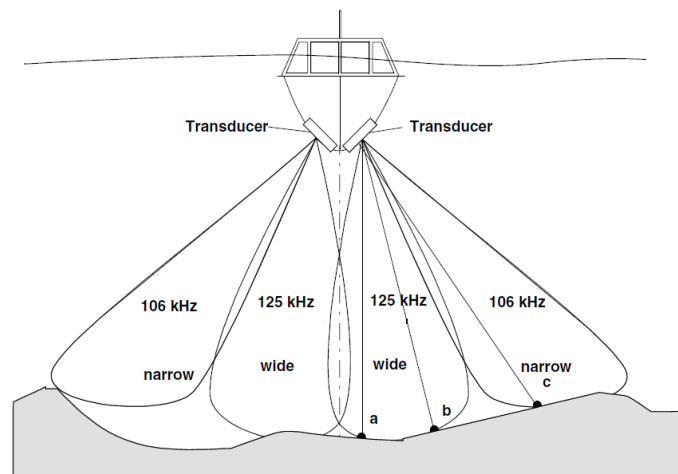


Figure 4.3: Orientation of the beams in the transverse direction[?]

4.1.2 Measurement process

Each part of the water bottom that receives sound from the transmission pulse sends back an echo of greater or lesser strength. An echo of this kind arrives at the reception staves at different times, depending on the direction of incidence of the sound.

From the sound travelling time from the transducer to the bottom element and back, the slanting range between the bottom element and the transducer can be calculated by means of the mean sound velocity, and finally the depth and the lateral distance can be calculated from the slanting range and the angle relative to the vertical. A necessary prerequisite here is that the sound velocity in the water at the location of the transducer must be known exactly, which means that the temperature, salinity and pH have to be determined in advance.

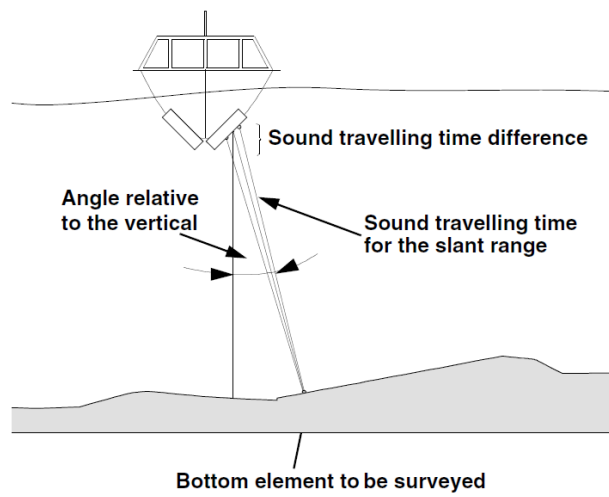


Figure 4.4: Measurement process[?]

4.1.3 Accuracy of the instrument

- **Measurement of Sound Velocity**

C-Probe determines the sound velocity directly by the measurement of sound travelling time (the "sing-around" method). If mud is deposited on the reflector of the sound travelling track, the track acts as if it has become shorter and the sound velocity value determined can be too high by a considerable amount. Therefore, for data collection, the probe must be cleaned before use.

- **Roll Angle Measurement with a Motion Sensor**

The longitudinal axis of the motion sensor should be arranged exactly perpendicular to the transducer beams. Because the dynamic measurement-error of the motion sensor is less than 0.05° , the angle error of the motion sensor should therefore be less than 0.3° . If there is a trim error (angle error), then when a ship is pitching, its pitch value acts to some extent as a roll error. If, on the other hand, the roll axis of the motion sensor is not exactly perpendicular to the transducer beams, which point in a direction transverse to the sailing direction, the pitching motion has an effect in the roll axis of the motion sensor, and causes a roll measurement error.

$$\text{Rollerror} = \arcsin[\cos(E) * \sin(\text{roll}) - \sin(E) * \sin(\text{pitch})] - \text{roll} \quad (4.1)$$

roll = true roll angle of the transducer

E = angle error of the motion sensor roll axis compared to the true roll angle

pitch = true pitch angle

- **Measurement of the Course Angle**

In the case of a multi-beam sweeping echosounder, the compass has the task of presenting a bottom detail, e.g. an obstacle, at the correct position in the coordinate system used. A compass installation error or a compass error in general, affects the coordinate offset of an underwater object in the sailing direction according to the following formula:

$$\text{Coordinateoffset} = \text{distanceoftheobject} * \sin(\text{compasserror}) \quad (4.2)$$

The offset perpendicular to the sailing direction can be ignored.

4.1.4 Inclination of the Transducer's Radiating Face Relative to the Horizontal (100 kHz)

If the specified maximum depth is utilized: 50°

In all other cases: 53°

50° angles of installation have the effect that the area vertically under the ship also produces strong echo levels. The coverage depends on the water bottom, and is often limited to just less than 6-fold, but in the case of mainly large measurement depths this leads to wide survey swaths for each track. In the case of sea surveying, where the roll errors of the motion sensor reach the order of magnitude of the FANSWEEP 20 measurement accuracy, larger coverages have a reduced accuracy.

4.1.5 Effects of different installation positions of system components

As the ship movement is related to the ship's center of gravity, all resulting movement, e.g. of the echosounder, need to be calculated. For this the positions of the echosounder and the motion sensor in relation to the ship's center of gravity needs to be known. More than this the axes of sensors should be aligned to the ship's co-ordinate system. The further away the motion sensor is installed from the echosounder, the more precisely the offset values have to be determined, because the size of the error has a linear, distance dependant effect.

The GPS unit is installed at a height of 17 m at the top of the research vessel. Motion Reference Unit is kept in the dry lab. Transducers are installed in the hull of the ship.

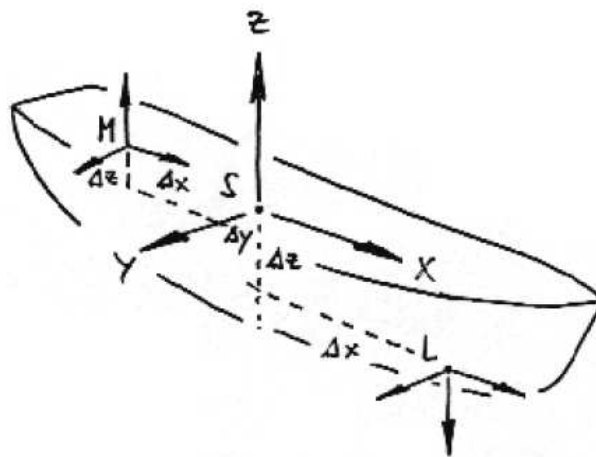


Figure 4.5: Relative positions of the system components[?]

4.1.6 Ship Movements

- **Heave**

Heave is a vertical translation along the z-axis. A varying coverage is always the result of heave. Uncompensated heave produces a constant depth error for the swath in the amount of the heave value.

- **Pitch**

Pitch is the result of a rotation of the ship around the transverse axis (y-axis). Uncompensated pitch produces an error in depth and position.

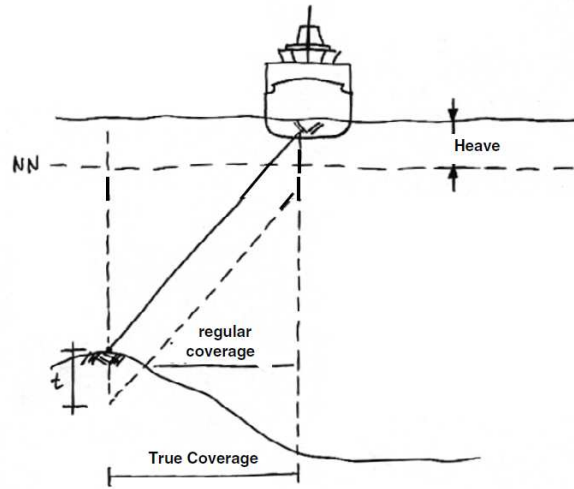


Figure 4.6: Heave[?]

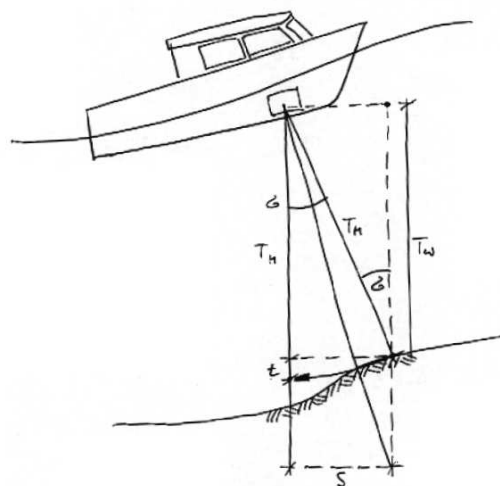


Figure 4.7: Pitch[?]

- **Roll**

Roll is the result of a rotation of the ship along the longitudinal axis (x-axis). Uncompensated roll produces an error in depth and position.

- **Yaw**

Yaw is rotation of the ship around the vertical axis (z-axis). Uncompensated yaw produces an error of the depth position.

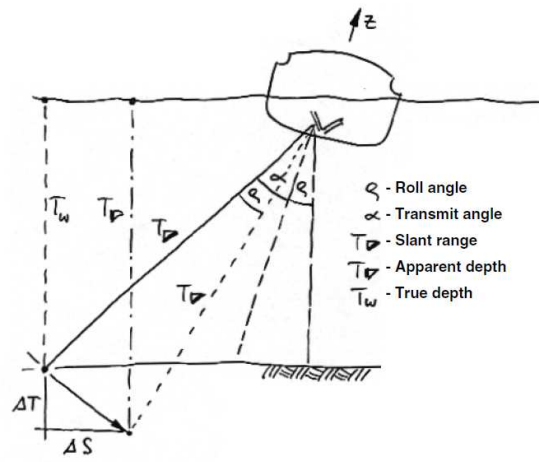


Figure 4.8: Roll[?]

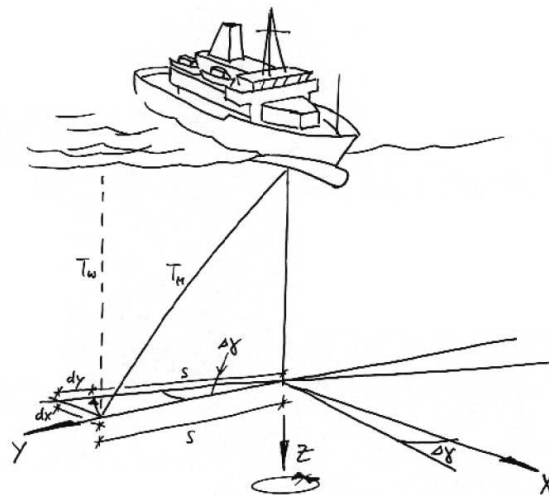


Figure 4.9: Yaw[?]

4.1.7 Coverage

The coverage is reduced, when the reflectivity decreases and the absorption increases. The pingrate decreases with increase in depths and coverages, because the traveltimes of sound on the outer beams increases.

4.1.8 Sound Velocity

A wrong sound velocity produces depth error and dislocation of the positions. If the setup value is less than the true sound velocity, then the depth calculated is too small and if it is greater than the true sound velocity, the depth calculated is too big.

4.1.9 Multibeam echosounder v/s Side scan sonar

Side scan sonar concentrates on the shadows being cast by its beam behind the objects on the sea floor, while Multibeam Echosounder (MBES) focuses on the resultant bathymetry for object detection. The low grazing angle of the side scan sonar beam over the sea floor makes it good for object detection. Though MBES gives us high-resolution bathymetry, still post processing of the data is required to visualize results. The advantages of MBES over side scan sonar are that the multibeam data is precisely georeferenced and the survey speeds are high.[?]

4.1.10 Method of data collection

As discussed in more depth in the next section, several variables affect the quality of the multibeam data including tides, salinity and pressure. Therefore, information for these variables needs to be collected so that it can be corrected for in post-processing.

Also, information on tides are needed to correctly interpret the acquired data. As the data was taken near the German island Helgoland, the tides recorded on Helgoland are taken as a reference to correct for the tidal offsets in height. The values for salinity and pressure were acquired by a CTD conducted on the cruise.

The Motion reference unit used on this cruise was the TSS DMS 2i. It corrects for roll, pitch, heave, and yaw which were explained in section ???. It started working effectively at 10:05 UTC time on Day 1.

Profile No.	Start Date Time[UTC]	Lon Lat[degrees]	End Date Time[UTC]	Lon Lat[degrees]	Average Speed[knots]		Filename
1 ^a	4.13.09 08:14:19	8.5779 53.5301	4.13.09 11:09:25	8.0923 53.8302	7.77	Helg1	11.09.2009_00F1090413
2 ^b	4.13.09 11:09:43	8.0912 53.8435	4.13.09 12:50:03	7.7577 53.9974	9.78	Helg2	11.09.2009_00F1090413
3 ^c	4.13.09 12:50:17	7.7577 53.9979	4.13.09 13:12:45	7.7571 54.0481	8.12	Helg3	11.09.2009_00F1090413
4	4.13.09 13:17:43	7.7590 54.0478	4.13.09 13:40:54	7.7578 53.9974	7.71	Helg4	11.09.2009_00F1090413
5	4.13.09 13:59:36	7.7563 53.9986	4.13.09 14:50:54	7.7804 54.0414	3.66	Helg5	11.09.2009_00F1090413
6	4.13.09 15:04:51	7.7825 54.0423	4.13.09 16:34:49	8.0646 54.0683	6.75	Helg6	11.09.2009_00F1090413
7	4.13.09 17:11:42	8.0844 54.0704	4.13.09 18:55:40	7.8943 54.1739	8.17	Helg3	11.09.2009_00F1090413
8	4.14.09 06:11:23	7.8985 54.1716	4.14.09 06:27:00	7.8938 54.1412	7.07	Helg8	11.09.2009_00F1090414
9	4.14.09 06:27:14	7.8936 54.1412	4.14.09 06:31:01	7.8938 54.1429	4.86	Helg9	11.09.2009_00F10904140
10	4.14.09 06:33:06	7.8811 54.1442	4.14.09 06:49:13	7.8447 54.1528	5.12	Helg10	11.09.2009_00F1090414
11	4.14.09 06:49:26	7.8443 54.1530	4.14.09 07:18:20	7.8367 54.1540	1.13	Helg11	11.09.2009_00F1090414
12	4.14.09 07:33:44	7.8494 54.1519	4.14.09 07:39:09	7.8351 54.1505	2.88	Helg11	11.09.2009_00F10904140
13	4.14.09 07:39:16	7.8349 54.1505	4.14.09 08:16:44	7.7392 54.1506	5.42	Helg13	11.09.2009_00F1090414
14	4.14.09 08:22:40	7.7387 54.1502	4.14.09 08:34:28	7.7390 54.1322	5.37	Helg14	11.09.2009_00F1090414
15 ^d	4.14.09 08:34:34	7.7390 54.1321	4.14.09 09:46:11	7.7394 54.1323	4.56	Helg15	11.09.2009_00F1090414
16	4.14.09 09:46:21	7.7397 54.1323	4.14.09 09:56:20	7.7676 54.1319	5.95	Helg16	11.09.2009_00F1090414
17	4.14.09 11:15:54	7.9642 54.1318	4.14.09 12:52:49	7.9613 54.2450	5.34	Helg17	11.09.2009_00F1090414
18 ^e	4.14.09 12:53:06	7.9612 54.2454	4.14.09 12:59:33	7.9632 54.2449	4.65	Helg18	11.09.2009_00F10904141
19	4.14.09 12:59:44	7.9628 54.2448	4.14.09 13:34:50	7.8952 54.2453	5.15	Helg19	11.09.2009_00F1090414
20	4.14.09 13:35:49	7.8765 54.2467	4.14.09 13:37:06	7.8772 54.2487	5.78	Helg20	11.09.2009_00F1090414
21	4.14.09 13:54:55	7.8778 54.2633	4.14.09 13:56:47	7.8780 54.2661	5.45	Helg21	11.09.2009_00F10904141
22	4.14.09 13:59:31	7.8801 54.2652	4.14.09 14:08:47	7.8797 54.2615	6.03	Helg21	11.09.2009_00F10904141
23	4.14.09 14:11:38	7.8820 54.2505	4.14.09 14:20:41	7.8820 54.2653	5.93	Helg23	11.09.2009_00F10904141
24	4.14.09 14:23:37	7.8841 54.2654	4.14.09 14:32:54	7.8838 54.2507	5.77	Helg24	11.09.2009_00F10904141
25	4.14.09 14:35:40	7.8865 54.2506	4.14.09 14:40:09	7.8848 54.2579	5.91	Helg25	11.09.2009_00F10904141
26	4.14.09 14:40:31	7.8847 54.2585	4.14.09 15:03:35	7.8204 54.2480	6.40	Helg26	11.09.2009_00F1090414
27	4.14.09 15:04:19	7.8182 54.2477	4.14.09 15:10:51	7.8007 54.2450	5.87	Helg27	11.09.2009_00F10904141
28	4.14.09 15:11:22	7.7998 54.2449	4.14.09 16:05:54	7.8980 54.1714	7.21	Helg28	11.09.2009_00F1090414

^aThere is a data gap from 09:04:01 to 10:05:56 due to resetting of the GYRO to correct the heading.

^bThere is a data gap from 12:24:37 to 12:46:29 as a result of the SURF data storage capacity being exceeded.

^cProfiles 3 and 4 were the calibration run.

^dNot a line but a big loop.

^eNot a line but a loop.

4.2 Data Processing techniques

To view the data recorded with the multibeam as an image, the data has to be processed. Processing is subdivided into pre- and post processing steps.

The first step of processing is pre-processing. Pre-processing transforms the raw data into .sda files. This is done on the computer devoted to the multibeam system and then the preprocessed data is transferred to challenger. One created .sda file comprises data collected by the multibeam over a period of 10 minutes. .sda files belong to the class of SURF files. SURF data files are 3D scanner files. The reason why SURF files are convenient to use in this case is the fact that they are open source and can be read by the program MBsystems, which is used for post processing and visualizing the data.

After the pre-processing, the data can already be visualized. Nevertheless it still has to be corrected for measurement error sources, which is called post processing. Post processing and visualization is done using software called MBsystems. MBsystems is an open source software package, which was developed for the processing and display of bathymetry and backscatter imagery data derived from multibeam, interferometry, and sidescan sonars.

The first thing the data should be corrected for is tides. As measurements are taken over a period of time, sea level height will vary due to the tides. This has to be corrected for to find the true depth at every point of measurement. Ideally, one has a tide timetable for every spot on the track, which one can subtract from the measurements taken. As this is not possible, because no such data is available, the data of the nearest location for which the tides are known is used. As the data during this cruise was taken around Helgoland, the tidal heights measured on Helgoland were used for correcting for tides. The program xtides was chosen to correct for tidal variations.

Another correction has to be made for the varying salinity and pressure conditions in the water column as they influence the velocity profile of the signal. Salinity and pressure conditions are usually unknown throughout the track. In this case, the salinity and pressure profile measured by a CTD during the cruise are taken and considered to be representative for all the area investigated.

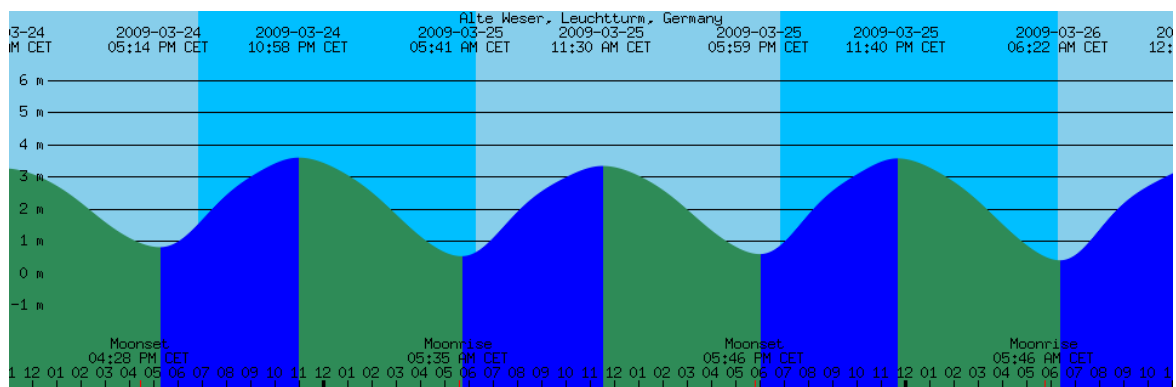


Figure 4.10: Example of the recorded tides which are used by the program xtides to correct for tidal offsets.

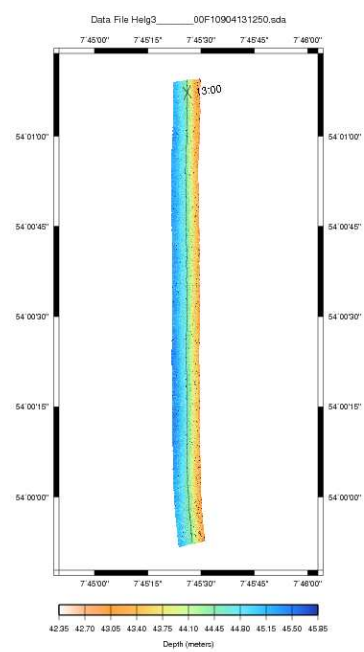


Figure 4.11: Calibration run going northward

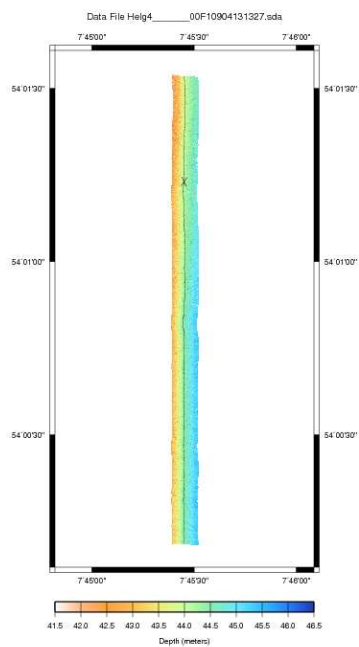


Figure 4.12: Calibration run going southward

As it is impossible to install the two transducers at a 50 angle by hand, one has to account for little offsets in the setup as well. This is done by calibrating the system. A calibration run is done by passing over a calibration area twice, but from different directions. The two images produced by the calibration run should give exactly the same result for the seafloor topography. As it can be seen in Figure ?? and Figure ??, this is not the case for these measurements, meaning that the transducers are not at a perfect angle. This can be corrected for by overlaying the results for the calibration run using the command `MBcopy` to figure out the offset-angle of the transducers. This angle correction can then be applied to all the data collected using the command `MBedit`.

In addition, the data has to be corrected for line drop outs, navigational errors and in this case the GYRO, which was not working in the beginning.

4.2.1 Results and analysis

By looking at first images, one notices that not only large scale features, but also small scale features such as shipwrecks are resolved very well on the multibeam image. In general, it appears that the seafloor is inclined, because the data has not been corrected for the angular offset of the two transducers yet.

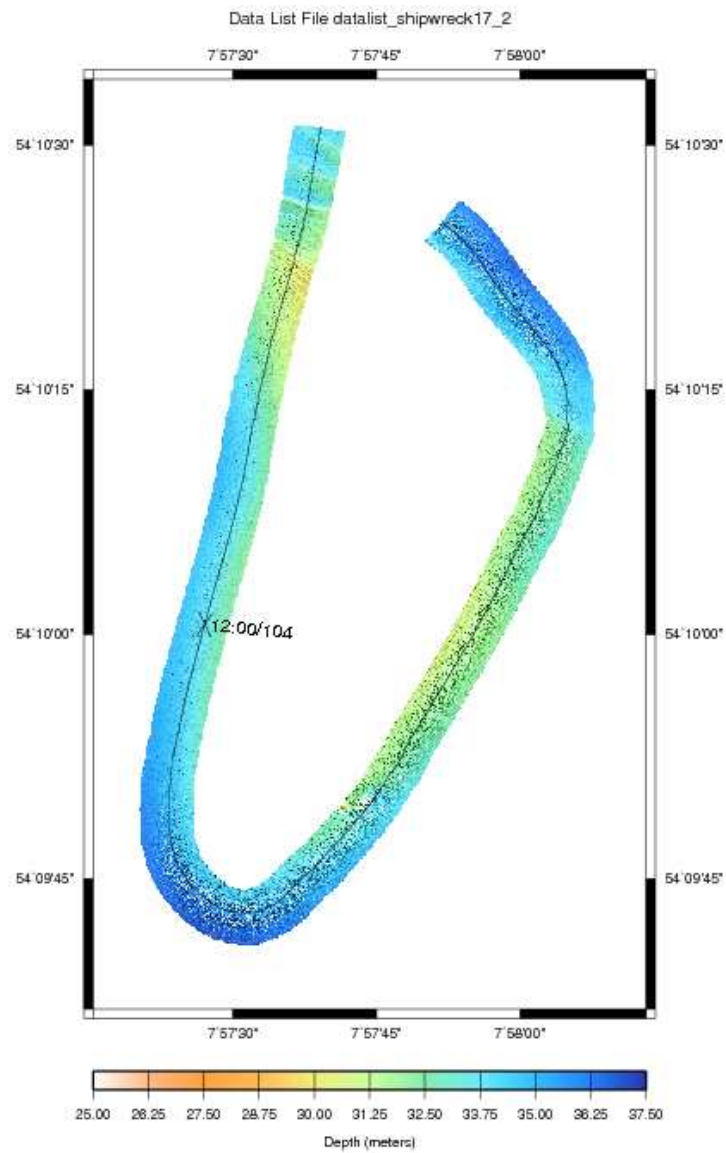


Figure 4.13: Sediment ridges in the north-west

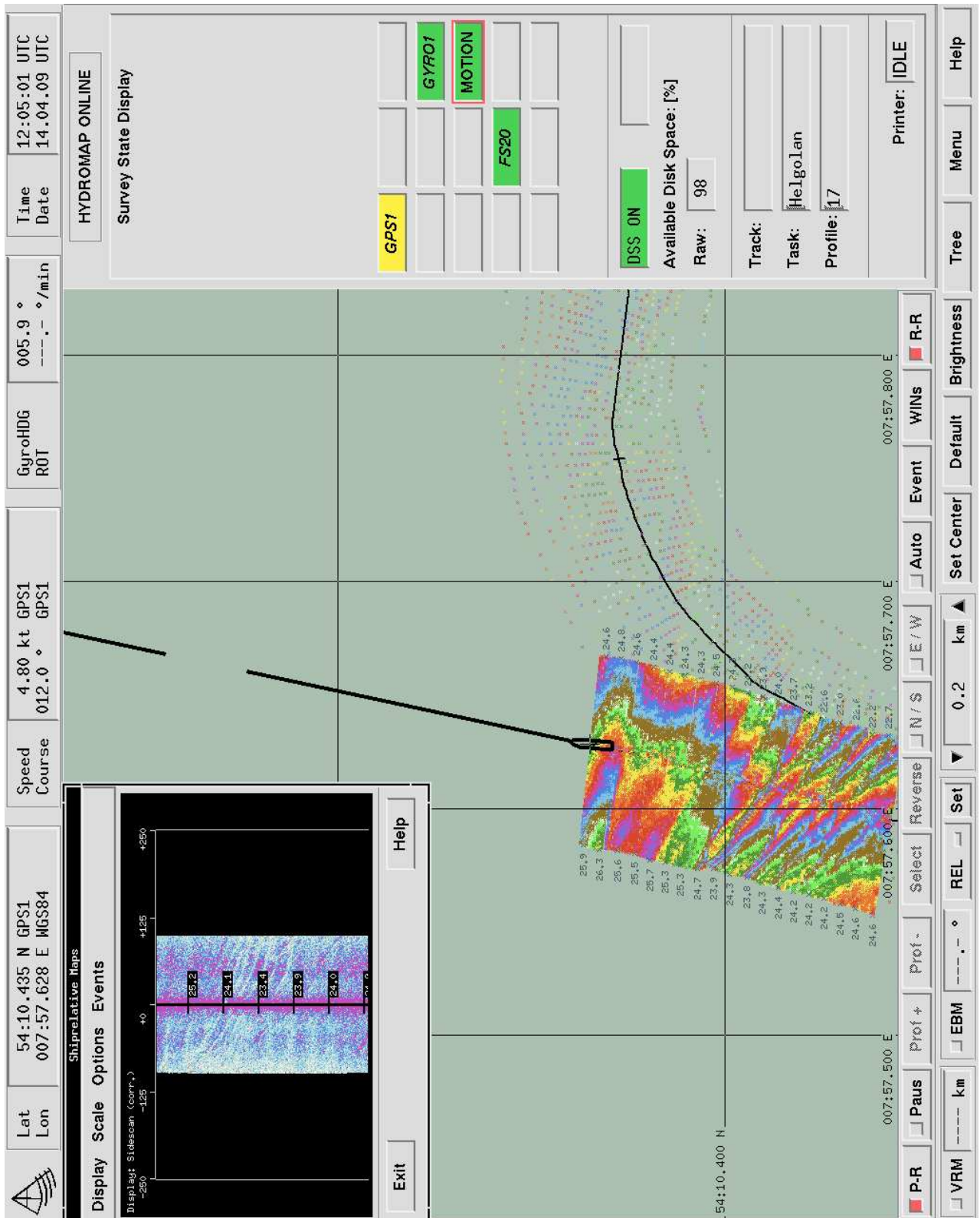


Figure 4.14: Screenshot of the data acquisition software showing the sediment ridges that can be seen in Figure ??

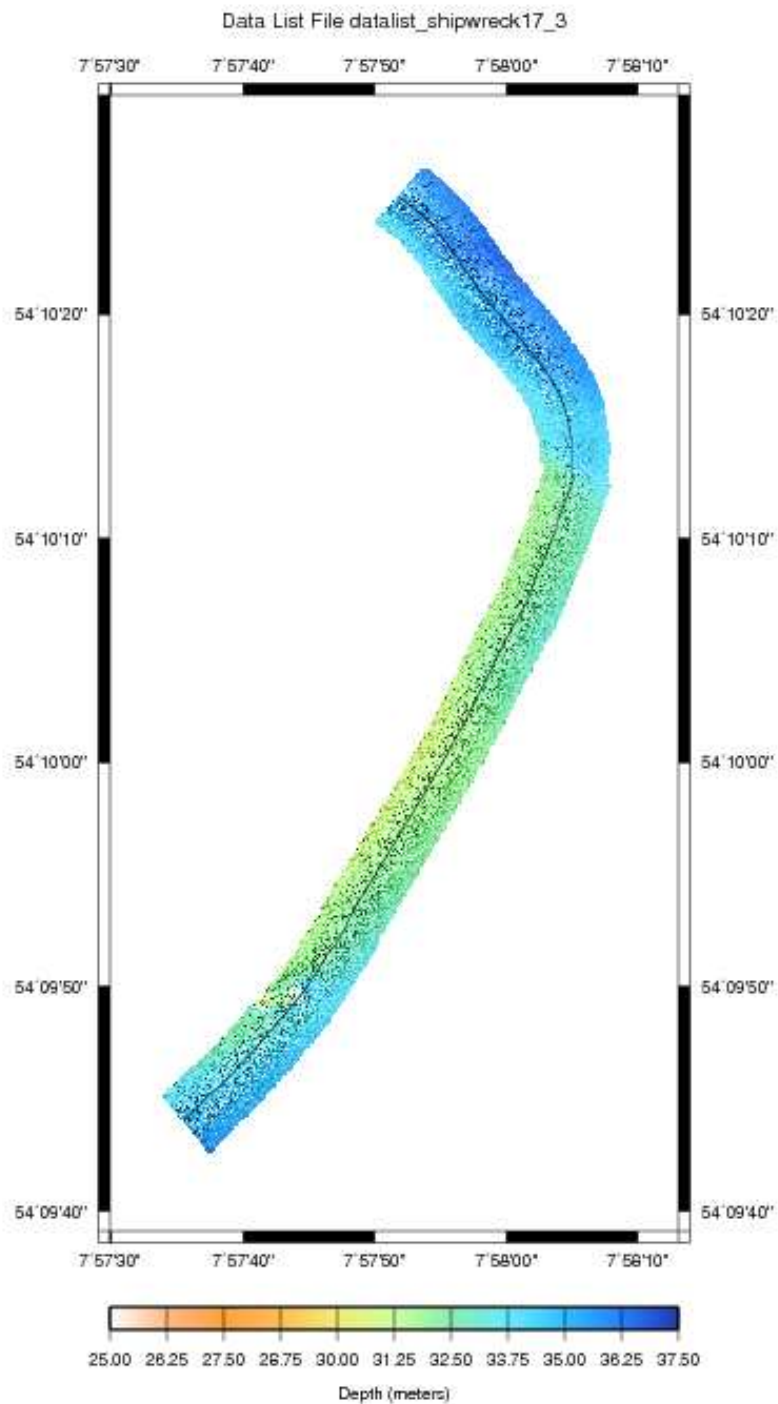


Figure 4.15: Shipwreck in the south-west at 54°09'50" N 7°57'45" E

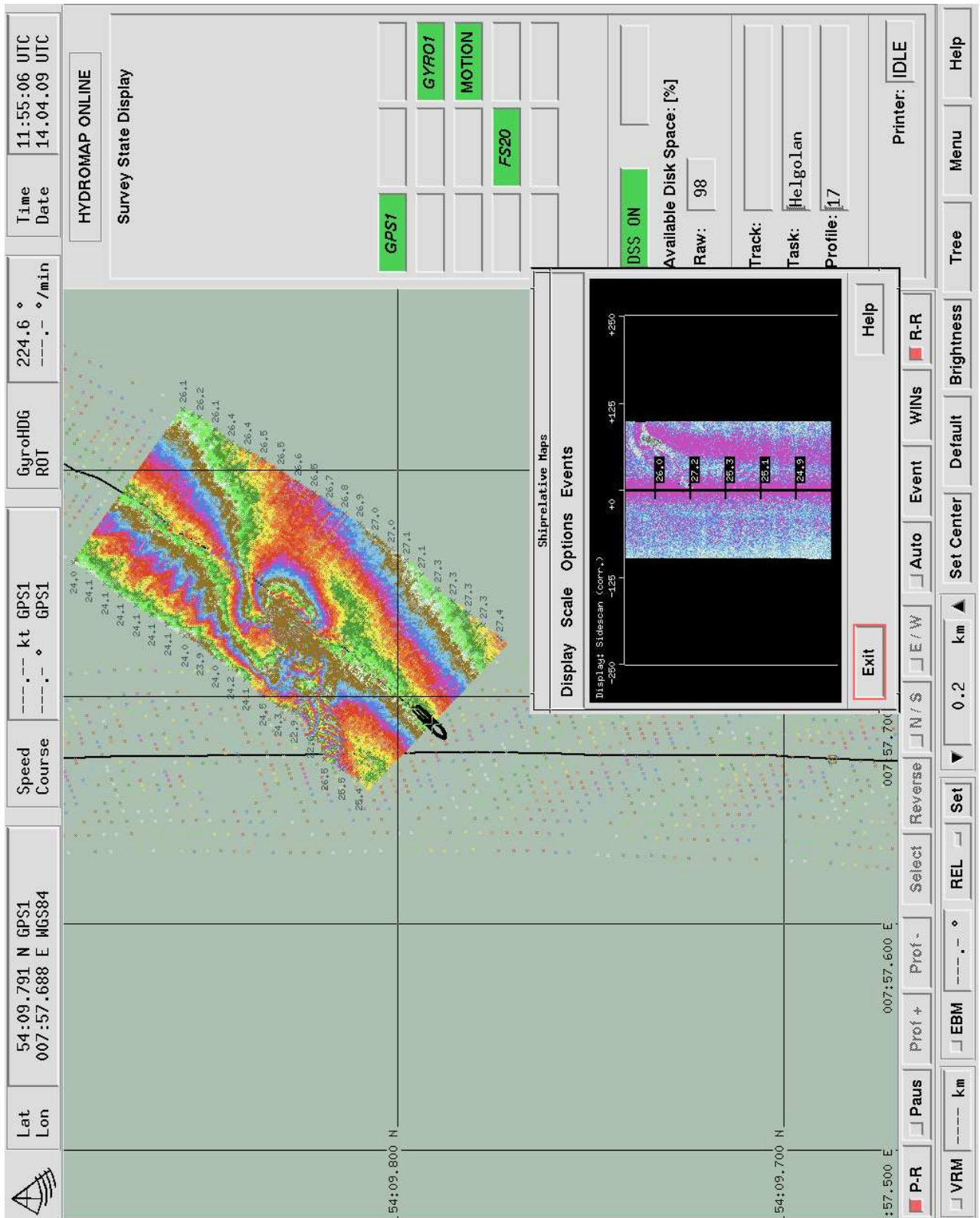


Figure 4.16: Screenshot of the data acquisition software showing the shipwreck that can be seen in Figure ??

4.3 Discussion and Conclusions

The data acquired seems to be of good resolution as even shipwrecks and sediment ridges can be seen clearly. It still needs to be corrected for height differences caused by tides and the angular offset of the transducers. Otherwise there seems to be no major error source as the multibeam system was set up correctly and all the instruments were delivering good results, except for the gyro in the beginning. This might be a little difficult to correct for. Nevertheless, the gyro was broken before the main area of interest was reached, so quality losses in that part of the data acquisition do not have severe consequences for the data. Also, there are two major data gaps in the beginning; one due to the resetting of the GPS to make the gyro work, the other one because all the data space on the hard disk was full and it had to be transferred to another computer. But those two gaps occurred before the main area of interest was reached and did not affect the calibration run. The data has to be corrected for tides, the angular offset of the transducers, line drop outs and navigational errors. After the processing has been completed, the data should be compared to already existing data. By doing so, one can look for major differences between the data set which would hint at a major error source which has not been accounted for.

All in all, one can conclude that the system worked well, except for some minor difficulties in the beginning. The data acquired is of good quality as it resolves even small scale features very well. Nevertheless, some processing work still has to be done on the dataset before it can be used for further research.

5 Sidescan Sonar

by Marta Gomez Betanzos

5.1 Aims

5.1.1 Instrument used, general principals of Side Scan Sonar

What is Side Scan Sonar

The basics of the Side scan sonar are the same as those of a normal sonar (sound, navigation, ranging). In this case, the side scan sonar is used to produce an image of the seafloor topography as well as objects on the seafloor, like boulders, shipwrecks, sunken objects, sediment ripples, fish and more while being towed from behind, at a fair distance from the propeller, or, preferably, at the side of the vessel a few meters (minimum 1 meter) above the sea floor surface. It is important that the Side Scan does not get too close to the seafloor, or else there is a risk of the tow fish hitting the ground and breaking off. None-the-less, the closer to the seafloor and the slower the vessel is moving the stronger the signal received and therefore the resolution of the scans. Side scan sonar is also referred to as side-looking sonar or side-imaging sonar. It can scan hundreds of meters of seafloor on both sides of the tow fish within real time while producing a near-photographic quality image of the seabed. It is referred to as "side" scan since it emits sound waves to the sea floor at an angle rather than straight down. (See figures 1 and 2, or a and b respectively)

Side Scan sonar has many uses other than research and science purposes, namely -commercial, military, leisure, detection of mines and fisheries, lost archaeological treasures and ship or plane wrecks among others.

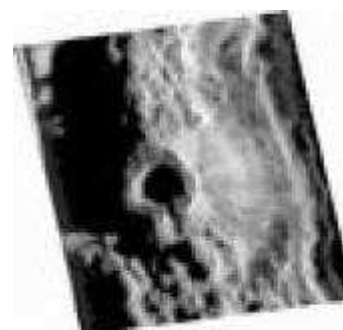
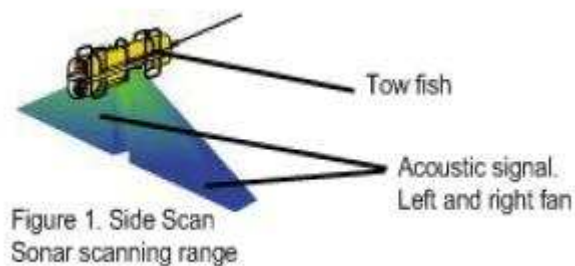


Figure 2. Side Scan image of a seafloor volcano, showing the different levels of signal intensity and the acoustic shadow of the outcrop.

Getting started

First thing one needs to do is to make sure everything is connected properly, with the exception of the Side Scan which should not be plugged in until it is actually being deployed. The items to be connected should be such that the power supply (for both the control box and the console), GPS cable, and Side Scan (later) are connected to the Side Scan surface interface SeaHub (the one receiving the raw data); the surface interface SeaHub is then connected to the console (toughbook) which then interprets the data transmitted by the surface interface SeaHub box. (See figure 3) After this has been done we secure the tow fish with the security hatch and safety pins so that they are fixed in place. The tow fish is now ready to be put into the water and start recording. It might be necessary to install SeaNet Pro into the toughbook to be able to receive, record and interpret the data.

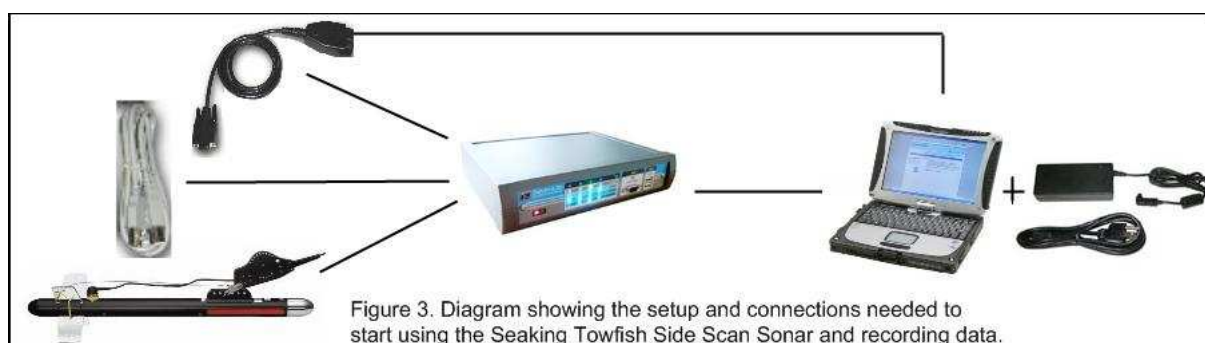


Figure 3. Diagram showing the setup and connections needed to start using the Seaking Towfish Side Scan Sonar and recording data.

How does it work?

Side Scan Sonar consists of a sensor head(s), a control and a display software. The head transmits both high and low frequency so that high frequencies will map the seafloor surface and specific structures and low frequencies sub-bottom imagery (depending on the type of sonar used, it is not always a given). As said above, Side scan sonar sends out a fan-shaped acoustic pulse which is perpendicular to the direction of movement. The signal travels through the water until it hits the seafloor or a solid structure(outcrop). The signal is then bounced off and recorded by the tow fish along with the travel time, amplitude and strength. These values are then sent to the console for further interpretation. In general terms, the console will use the values to produce a long continuous image of the mapped seabed (stored as .v4log files) as well as a real time grey-scale image of the seafloor. The stronger signals will be shown as white areas, while the weakest, or zero, signals as shown as black; the rest are scaled accordingly. (See figure 2) Strength of signal is defined by the slope and the structure or material of the seafloor; so that stronger signals will be received when the seafloor slopes towards the tow fish and is made of bare rock. In contrast, weak signals will happen when the seafloor is covered with mud or sand and slopes away from the tow fish emitters. Furthermore, the image will also show the shadows of the structures similarly to that of a flashlight shining on the structure. (See figure 2) This is usually referred to as the *acoustic shadow* of the object being mapped. (See Figure 4)

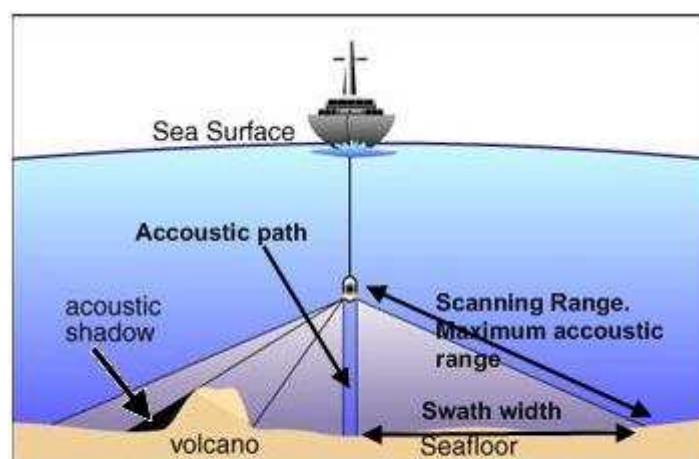


Figure 4. Graphic sketch of a Side Scan Sonar being towed behind the ship.

Working with the console. The toughbook

The most basic buttons when working with the toughbook are those that deal with the image resolution of the raw data received from the Sonar. (See figure 5). Starting from the left we have the setup menu which is self-explanatory, but will also be explained in more detail below. The on/off/pause button which starts, stops or pauses the data recording and image production (interpretation of data by the console); then the channel gain for both the left and right side of the Sonar which set the Sonar receive gain and display contrast, so how sensitive the sonar receptor are to the receiving signal and the scale (in dB) or level of saturation. Sonar channel gain is usually set to 40% although it depends entirely on the water conditions and on the type of sediment of the seafloor. Sonar display contrast also vary depending on the water conditions, though mostly on the speed of the vessel; such that one must pay attention that the dB indicators on either side are always larger than the red (left) and yellow (right) markers to avoid oversaturation of white. Next are the range, which defines the area of seafloor the Sonar beam covers/scans, the resolution and the Frequency display. The resolution varies from low (Lo) to high (Hi) even ultra (Ult) if one wants a very detailed scan image of the seafloor, otherwise Med (medium) or Hi are the typical settings. As for the Frequency, the typical value is 325Hz, and it defines the strength of the outward signal.

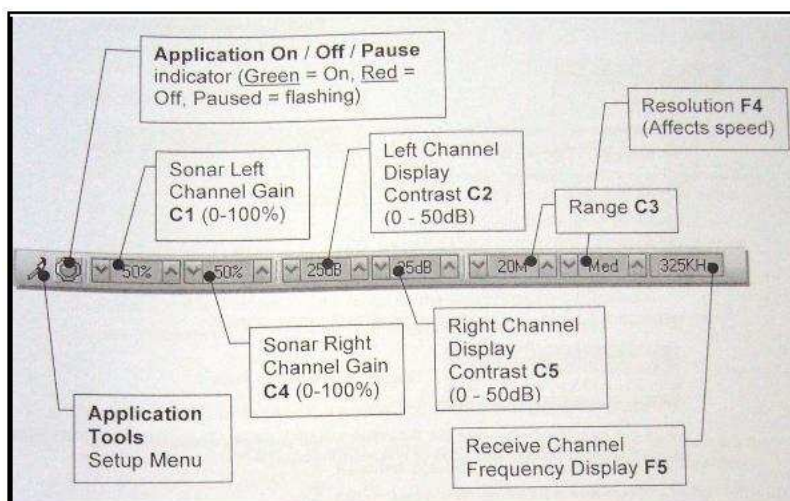


Figure 5. Basic buttons for working with Side Scan Sonar console and the data.

Some main features of the setup button mentioned above are the Cursor, Position and Setup options. The cursor option tab brings out a box showing the range, data and time of a specific point on the Side Scan waterfall image. The position option tab sets the layback distance in meters between the tow fish and the vessel. Finally the setup option tab allows you to define several parameters like the intensity sampling of Sonar data, painting the leading edge of strong targets to emphasize sub-bottom layers, the units of display or the number of range 'bins' sampled to the screen resolution. The range 'bins' are the sampled intervals; so every how many pulses the data is recorded, or in other words how often the received signals are sampled.

Interpreting Side Scan data images

So we know that only echoes of objects that reflect sound are recorded by the Side Scan sonar transducer. Burnished or smooth surfaces and finer sediments may not show too well on the echo image in a way that they may wipe out data from smaller structures nearby. In this way, clay and silts will be just barely visible (low backscatter) as opposed to metals, boulders, gravel or recently extruded volcanic rock which will give a high backscatter. Furthermore, if the side scan is being towed too fast the signals will not be received as nicely as when towed at slower speeds. Other than that, data from texture, structure and size of the objects is very nicely recorded and reproduced by the console. Knowing the strength of the receiving signal, one can examine the composition of the seafloor and any other structures or object. A sketch of a typical Side Scan sonar scanline would be as shown in figures 6 and 7, or a and b respectively.

Interpreting Side Scan sonar data is something that comes with experience and practice, and while reflections of small objects are harder to interpret, man-made structures like platforms or rock walls are easier to interpret due to their regular patterns.

The bottom line of using and interpreting Side Scan Sonar data is that you have to approach it as if looking at the world through a shiny black plastic with a flashlight's torch beam as the only source of light. Regarding the maintenance, it is important to wash the instrument (cable and tow fish) with fresh water after each deployment, making sure that it is rinsed properly of all (or most of) the salt water. Furthermore, the instrument, namely the tow fish, should not be exposed to extreme conditions.

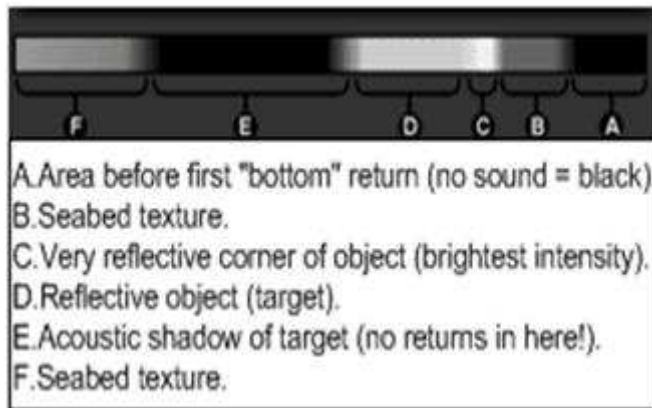
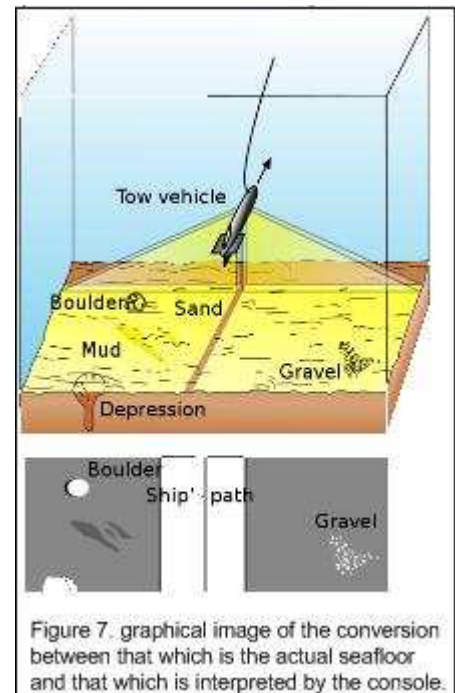


Figure 6. Example of a typical Side Scan Sonar scanline



Advantages and Limitations to Side Scan Sonar

Side Scan Sonar is a very useful tool for mapping the seafloor, especially in turbid waters, since structures, sediment types such as mud, sand, ripples, outcrops, boulders, canyons, buried objects, and even fish can be detected. Dense objects like rocks, coarse sand and metal will be reflected best by giving off a stronger signal; soft features like mud, sand, silt produce weaker signals since they actually absorb the sonar energy. However, regardless of its qualities Side Scan Sonar also has some limitations, -namely those related to the depth, strength of signal, data collection and interpretation, and resolution of the image produced based on the conditions of speed and distance to seafloor.

5.1.2 Method of data collection (list of line and line numbers collected)

Stations of Line	Line No.	Date	Start Time	Lat. & Long.	End Time	Lat. & Long.	Filename(s)
4 - 5	0	13 April	15:11	54°2.573" N 7°47.515" E	16:51	54°4.398" N 8°7.108" E	Mon_13_Apr_15_19.V4log 16-59-58.BMP
1 - 2	1	14 April	6:29	54°8.541" N 7°53.230" E	6:49	54°9.198" N 7°50.562" E	Tue_14_Apr_06_29.V4log
3 - 4	2	14 April	7:39	54°9.017" N 7°49.956" E	8:17	54°9.043" N 7°44.237" E	Tue_14_Apr_07_39.V4log Tue_14_Apr_08_08.V4log
4 - 5	3	14 April	8:18	54°9.112" N 7°44.180" E	8:34	54°7.887" N 7°44.344" E	Tue_14_Apr_08_18.V4log
7 - 8	4	14 April	9:50	54°7.938" N 7°45.050" E	10:58	54°7.971" N 7°57.903" E	Tue_14_Apr_09_50.V4log Tue_14_Apr_10_43.V4log
9 - 10	5	14 April	11:21	54°8.422" N 7°57.723" E	12:52	54°14.707" N 7°57.632" E	Tue_14_Apr_11_21.V4log Tue_14_Apr_11_40.V4log Tue_14_Apr_11_54.V4log 11-40-42.bmp Tue_14_Apr_12_20.V4log 11-46-41.bmp 12-34-35.bmp
10 - 11	6	14 April	12:53	54°8.422" N 7°57.723" E	12:59	54°14.707" N 7°57.632" E	Tue_14_Apr_12_53.V4log
11 - 12	7	14 April	12:59	54°14.676" N 7°57.060" E	13:33	54°14.800" N 7°52.597" E	Tue_14_Apr_12_59.V4log Tue_14_Apr_13_33.V4log 12-00-53.bmp
12 - 13	8	14 April	13:35	54°14.796" N 7°52.592" E	13:40	54°15.292" N 7°52.740" E	Tue_14_Apr_13_35.V4log 13-37-28.bmp
13 - 14	9	14 April	13:40	54°15.292" N 7°52.747" E	13:43	54°15.176" N 7°52.811" E	Tue_14_Apr_13_40.V4log
14 - 15	10	14 April	13:45	54°15.129" N 7°52.807" E	13:56	54°15.897" N 7°52.667" E	Tue_14_Apr_13_45.V4log
15 - 16	11	14 April	13:56	54°15.942" N 7°52.669" E	14:09	54°14.999" N 7°52.755" E	Tue_14_Apr_13_56.V4log
16 - 17	12	14 April	14:10	54°14.956" N 7°52.839" E	14:20	54°15.850" N 7°52.814" E	Tue_14_Apr_14_09.V4log 14-19-31.bmp
17 - 18	13	14 April	14:23	54°15.820" N 7°53.058" E	14:32	54°15.080" N 7°53.029" E	Tue_14_Apr_14_23.V4log
19 - 20	14	14 April	14:33	54°15.028" N 7°53.130" E	14:40	54°15.456" N 7°53.088" E	Tue_14_Apr_14_33.V4log
21 - 22	15	14 April	14:41	54°15.545" N 7°53.049" E	15:11	54°14.696" N 7°48.027" E	Tue_14_Apr_14_40.V4log 14-52-25.bmp

Figure 5.1: Table with the results obtained for April 14th showing start date, time and Latitude (Lat.) and Longitude (Long.) End date, time and Latitude (lat.) and Longitude, and file(s) corresponding to each line. Each line was done with the tow fish at 28 marks distance (with two marks having a distance of 1 meter) from the side of the vessel. Start time and end time were taking from the Console UTM; real time is 2 hours more of that shown on the table.

5.2 Data Processing Techniques

In our case the data was collected by using a Tritech SeaKing Towfish Side Scan Sonar System (toughbook console, interface surface SeaHub box, Side Scan and corresponding cables (side scan, power supply, GPS)). For the most part the general conditions were:

- Left gain and display contrast: 44-53% (namely 44%, 50% and 53%) and 47dB
- Right gain and display contrast: 41 - 67% (namely 41%, 47%, 63%) and 47dB
- Range 100 m or 200 m
- Resolution: Ult
- Frequency: 325 Hz

The parameters, -namely the left and right channel gain and display contrast-, had to be changed according to the vessel's speed, so that there were not any areas of white oversaturation or to avoid horizontal lines cutting across the data and giving "bad" data. Furthermore, the tow fish had to be pulled up sometimes to avoid it getting too close to the seafloor. During the stops for CTD, sediment samples, or when the small boat was launched and the vessel was stopped, the Tow fish had to be pulled in beforehand so that it did not get caught in the propeller or hit the seafloor. All data were collected on the 14th April, with the exception of the practice line (line No. 0) which was done on April 13th. Lines were named by the captain of the vessel according to the trajectory defined by the Navigation group. Due to the extremely large size of the data files, the lines had to be stopped and restarted every so often to avoid having huge unreadable files. The data was saved as .4vlog files and then converted to .XTF, .TIF (.GEOTIFF), and if possible to .KML (for Google Earth viewing). Looking at the display window data on the seafloor, sediments and outcrop structures were recorded to the sides leaving a blind band of data which was the area directly underneath the Side Scan. This area is really important to have under more or less constant surveillance, since it will tell you how close the tow fish is to the seafloor, and therefore warn you in case you have to pull it in a bit. Basically, what happens is that if the middle of the Side Scan path (a.k.a the vessel's trajectory line) and the first line of receiving signals come close together then the tow fish is practically on the seafloor and needs to be pulled in urgently. Take for example the following screenshot (see figure 13):

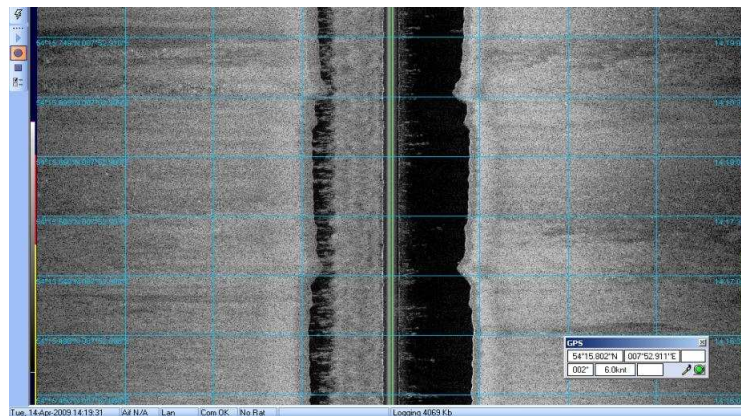


Figure 13. Screenshot of console display window showing a seafloor ridge.

Notice how, when the Side Scan passes next to a hill or a big ripple-like structure, the distance between the green center line and the seafloor surface becomes smaller. If the distance was smaller, so the seafloor and the green center line were closer together, then the tow fish would have to be pulled in a bit to avoid crashing it into the seafloor.

5.2.1 Results and Analysis

The data was collected in an area of the North Sea just off the coast of Helgoland on April 14th, starting 8:29 until 17:11(6:29 and 13:11 UTM). A total of 15 lines plus a 0 practice line were recorded. The Side Scan was previously set up according to the established procedure and then put in the water at a distance of 28 marks. Resolution of the image varied according to the speed of the vessel, although it was general set at a reasonable pace so that rather sharp images were obtained. The weather conditions were very nice, making the data collection all the easier and the results all the more clear. Major observations were a shipwreck (see figure 8), a depression or another shipwreck (see figure 9), sediment ripples (see figure 10), various types of sediments (see figure 11), boulders and fish (see figure 12), and seafloor hills or mounts (see figure 13).

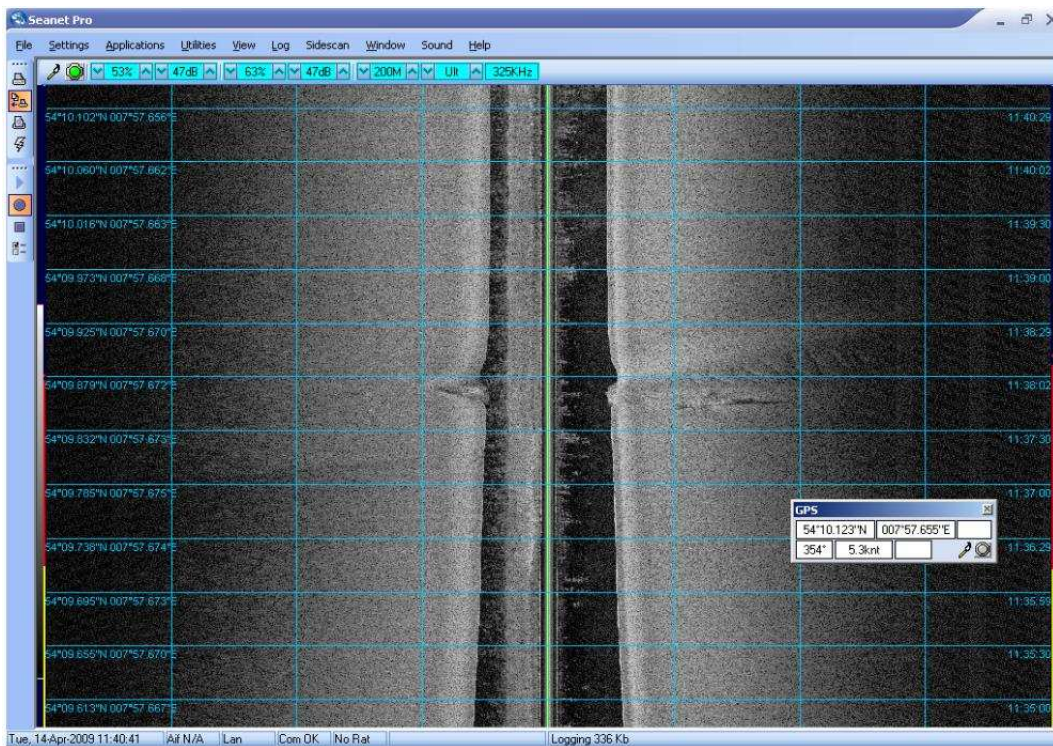


Figure 8. Screenshot of the Display window in the Console showing a shipwreck.

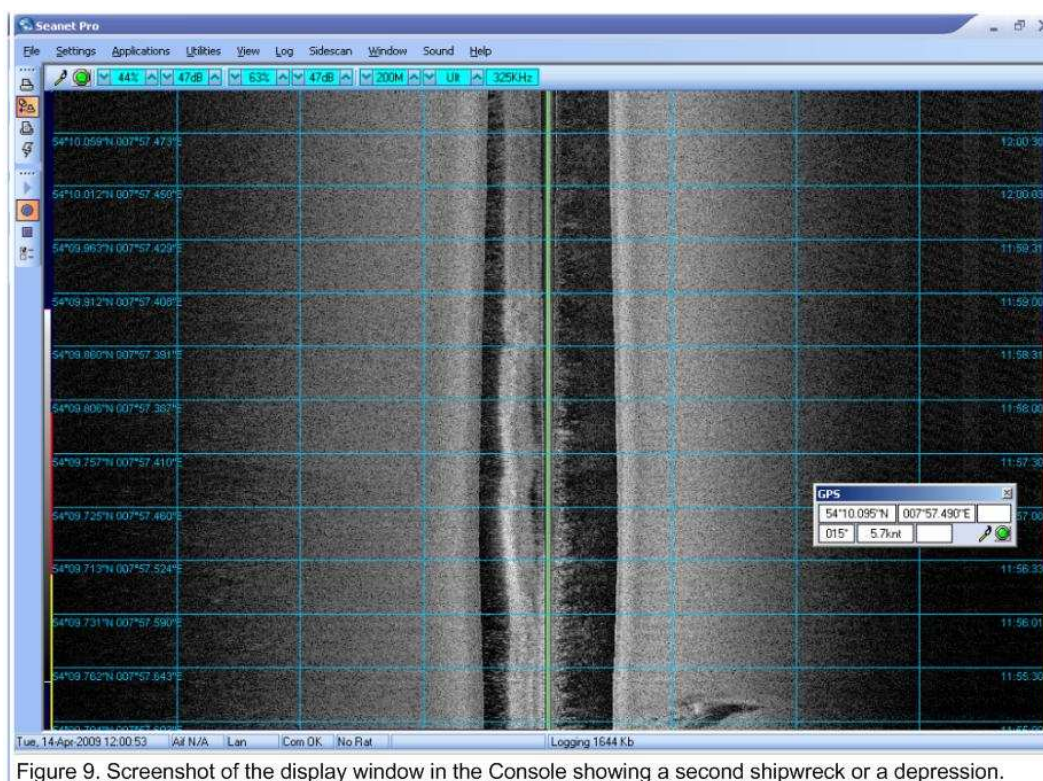


Figure 9. Screenshot of the display window in the Console showing a second shipwreck or a depression.

Figures 8 and 9 show what is definitely a shipwreck in figure 8 and what might be a shipwreck, a sunken object or a depression in figure 9. Observe how in figure 8 the bow and stern of the sunken ship are clearly distinguishable. Furthermore, the trace of the trajectory it followed at the time of sinking is also observed in the surrounding dent on the seafloor sediments. The middle part of the ship is within the Sonar's "blind spot", so that no data, and therefore image, was obtained.

The same more or less applies for the structure in figure 9, although in this case it is less obvious what it is. The problem here was that the console froze and this was the only data that was recorded. None-the-less, we can see the acoustic shadow of what looks to be obviously some sunken object, whether it be a ship or something else, or a depression in the seafloor surface.

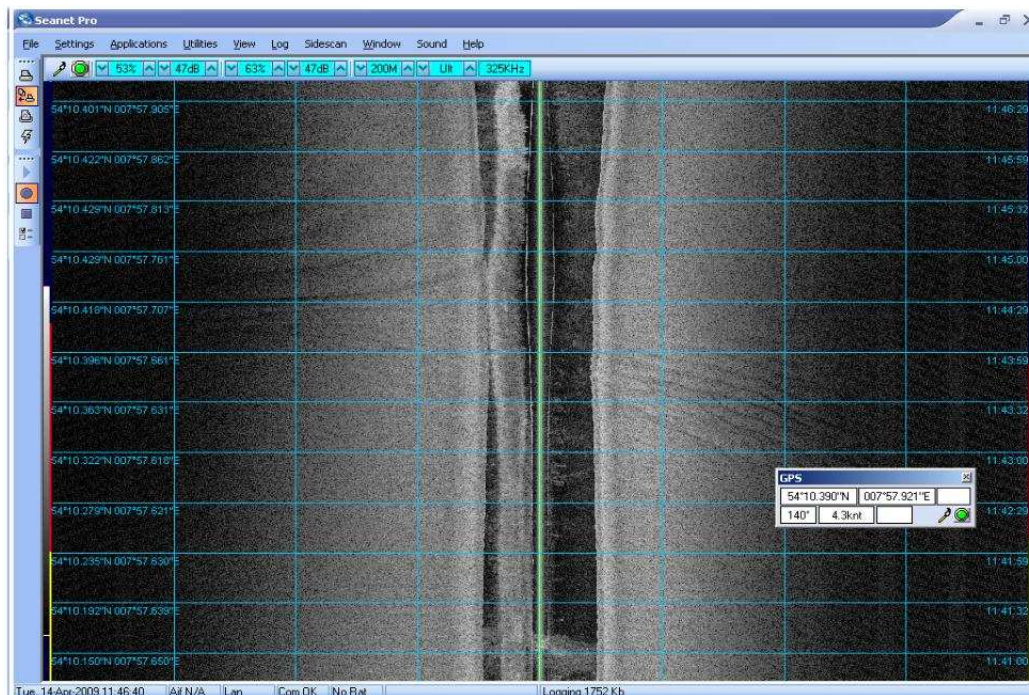


Figure 10. Screenshot of console display window showing clear sediment ripples especially on the right handside.

Figure 10 shows very nice sediment ripples on both sides of the Side Scan Sonar. Notice the lighter areas corresponding to the stronger signals bouncing off the top of the ripples and off the slope facing the Side Scan. The darker bands correspond to the backside of the sediment ripple where the frequency signals either do not reach or simply bounce off in directions opposite to the Sonar's receptors. It is also shown that there is a slight elevation of the seafloor since the Side Scan blind spot is temporarily narrowed down.

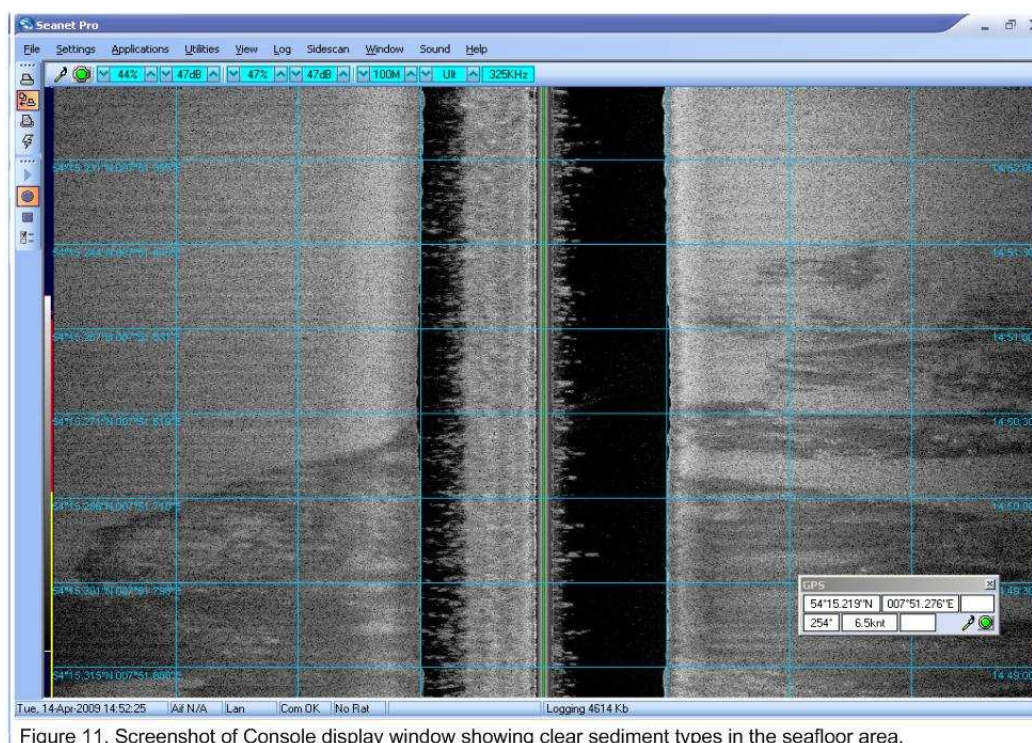


Figure 11. Screenshot of Console display window showing clear sediment types in the seafloor area.

In figure 11, very clear sediment types are visible. Considering that lighter areas correspond to stronger signal reception and that strong signals are typical of harder sediments, like rocks, coarse sand, metals, boulders, gravel or recently extruded volcanic rock; then we can assume that it has to be one of those; although it is most likely coarse sand, rocks and boulders (which we actually saw (see figure 12)) or gravel for the lighter colored patches and mud or silt for the darker patches.

As mentioned above, one of the sediment structures of the area has to be composed of boulders, since otherwise a weaker signal would be received and shown accordingly on the image. Proof that boulders are part of the sediments in the area covered is shown in figure 12, where we see lighter spots with the corresponding acoustic shadows which correspond to boulders on the seafloor. These lighter areas show higher surfaces which stand out from the seafloor surface as outcrops. Furthermore, the acoustic shadow only serves to give even more proof that there is an outcrop or some sort of structure standing out from the surrounding smooth seafloor surface. Also in figure 12, we can see some fish swimming within the Side Scan's "blind spot". Still using some of the old technology present in the traditional depth sounders, side scan sonars can still receive signals coming from directly below the tow fish. Fish, as any other object will reflect and send signal back to the sonar's receptors. The fact that there is a so-called "blind spot" right under the sonar means only that the signal received will not be as accurate as those bouncing back from object located to the sides of the sonar's path. Initially the Side scan sonar was also used to receive signals from directly below it, but with the development of the sonar technology the traditional single-beam depth-sounder was replaced by the side scan sonar, which "specialized" in listening to the echoes received from either side of the tow fish and not so much on what is directly beneath it. In time, the development of the multi-beam made this distinction less meaningful. Regardless of, side scan sonars also pick up on what is present in the water column, so any small grey-ish areas are all the small particles and organisms (such as fish or plankton) found in the water column.

Finally, figure 13 shows some clear seafloor hills that tend towards the Side Scan's trajectory, implying that we are probably cruising right on top of them; which is also why only half of the hill is visible. Here too the slope that tends towards the direction of the Side Scan (so facing it) is shown as lighter colored whereas the acoustic shadow where no data is received is shown as dark areas. One could also argue that, due to the obvious symmetry between the four larger peaks, the so-called hills could be either an agglomeration of sea mounds or two rows of individual sea mounds running almost parallel to each other. But that sounds like too much coincidence. It could also be that the tow fish went over what would be a ridge, or sediment waves. Looking at the image (figure 13) one can distinguish some darker areas which are slightly more elevated and which lead to the so-called hills. Due to the symmetry in the bumps it seems more probable that they are parts of a ridge.

Also in the screenshot are traces or marks of different sediment types.

Some examples of survey lines that were able to be converted to .TIF (or .GEO-TIFF) via the program Seanet Dumplog are:

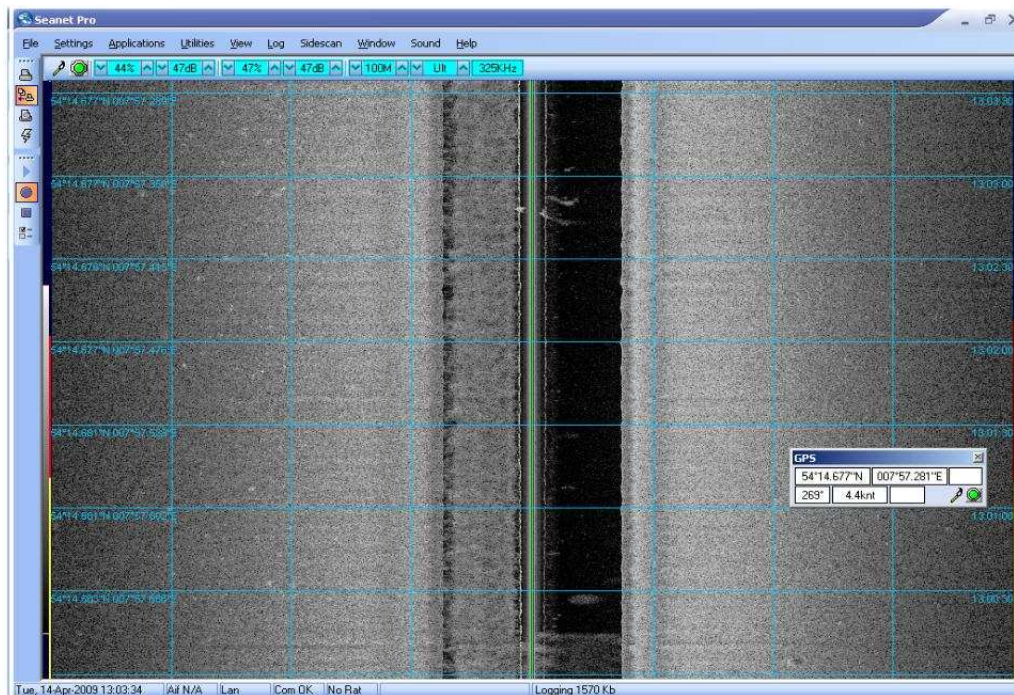


Figure 12. Screenshot of Console display window showing boulders (shown as white spots on the grey background) and some fish (shown as a grey oval shape within the Side Scan Sonar's and vessel's path; this could be because fish send out frequency signals which are received by the Side Scan as part of the signals it sends out.

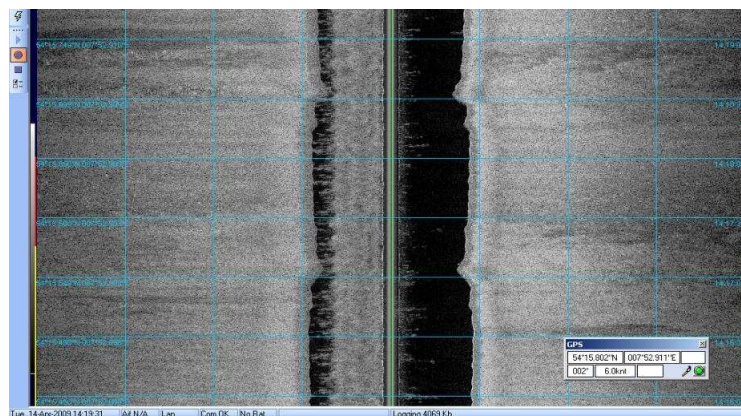


Figure 13. Screenshot of console display window showing a seafloor ridge.

Figure 2 shows what a typical survey line looks like. No major features are observed, but it is still a very nice survey line to have as an example. Some hills and ups and downs of the seafloor are visible.

On the left-hand side of this survey line (figure 3) we can see the seafloor hills, mounds or larger ripples explained before for the screenshot for figure 13. Black lines tend to represent missing or bad data. However, the appearance

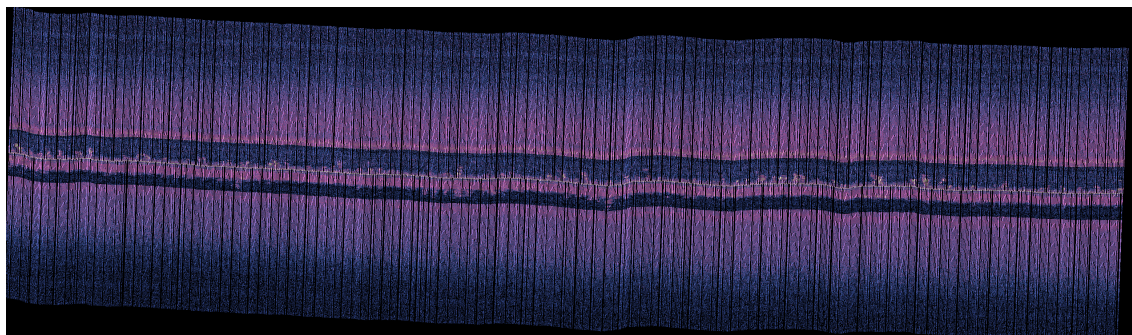


Figure 5.2: Side Scan Sonar survey line data file (.v4log) as an image file (.GEO-TIFF).

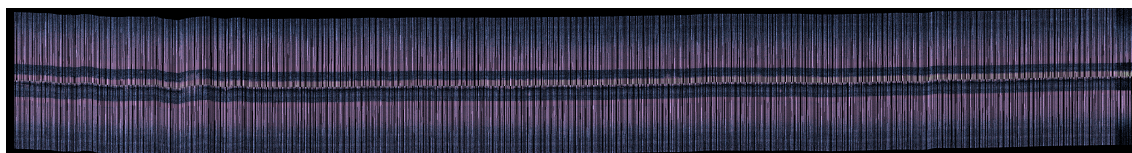


Figure 5.3: Side Scan GEOTIFF image showing some seafloor hill-like structures to the left-hand end of the image.

of major sections of bad data were rare and only on counted occasions.

Survey line Tue_14_Apr_12_59.TIF (file surveyline_10_43.eps) appears to be too large to be worked with in latex; none-the-less it has been uploaded with the rest of the data files in the challenger folder. The .GEO TIFF image shows what in figure 11 were described as different sediment types along the line going from 429068.327E, 5998787.195N to 4322395.91E, 5998798.946N. They appear as lighter colored areas (light green-yellowish areas) showing that there is a change of the receiving signal strength, which in turn implies a change in seafloor composition.

5.3 Discussion of some of the features observed

Some of the most interesting features observed in the course of the day were the very obvious shipwreck, the sunken object which was said to be another shipwreck although less obvious, the sediment ripples and types, and the seafloor hills. Some boulders and fish were also observed, but not too clearly. Regarding the first shipwreck (see figure 8) one could see a clear image of the bow, stern and dent on the seafloor of the ship. Judging from the dent on the sediment we can theorize how the ship sunk, or on the bottom water current; the direction in which the ship is given by where the bow is pointing as well as by the change in depth of the dent on the seafloor. Furthermore the same grey-scale image on the Side Scan console was obtained with the multibeam, although in this case the different heights showed up as different color layer instead of the grey scale that accompanies the signal strength of the Side Scan Sonar. The same was observed for the second so-said shipwreck, although one would be more inclined to say that it is simply some sunken object which due to punctual malfunctioning of the console was just barely observed (see figure 9). In this case the deeper areas surrounding the object are clearly visible; matter-of-fact, since there is a darker area enclosed between two lighter areas one would be tempted to say that it is rather some sort of depression in the seafloor, be it by the impact of some heavy object or due to biological or geological process; although once more this is only another hypothesis for the observed data. As with the previous case, the multibeam also registered it as a colored image showing heights via a color scale instead of in a grey scale. Still on the seafloor surface, we also saw some hills or mounds on the inner rim of the Side Scan Sonar acoustic signal fan. This implies that, as said above, the Side Scan cruised right on top of them, thus only capturing half of the hilly structures. We know that they are hills or mounds since surface height increases, making the Side Scan acoustic fan temporarily larger due to proximity to the seafloor. Also if one looks at the data (see figure 13) it is obvious that there is some sort of outcrop rising above the seafloor surface. Another hypothesis is that the observed hilly structures are really the ends of a small like ridge on the seafloor, some sort of larger sediment ripple-like structure. This is also possible, since if we take a close look at the figure, we see that the same structures show on both sides of the Side Scan at more or less same latitude, as if parallel to each other; suggesting the start and end points of a ripple-like structure like those observed in figure 10, although these are smaller more abundant ripples most probably formed by seafloor waves due to movement of water masses near the seafloor.

Moving into the sediment, just slightly below the seafloor surface, we see that the Side Scan actually picked up on different types of sediment compositions. This is very clear in figure 11, where different grey-scales define the strength of

the signal and therefore the hardness or softness of the sediment scanned. In the case of figure 11, we see lighter patches which most probably correspond to harder more reflective sediments such as gravel, rock, or coarse sand. On the lower part of the image and in between some of the lighter patches, we see darker areas which correspond to soft sediments; such that the signals were absorbed by the sediment instead of completely reflected. This then suggest some type of clay/mud, silt or fine grained sand. It was said that some boulders and fish were observed, but as explained above they were not very clear. The boulders where seen as small lighter shaded areas with their corresponding acoustic shadow, and the fish were seen as isolated signal reception within the Side Scan path.

5.4 Conclusion

The Side Scan Sonar was created in the 1950's for military purposes by German scientist, Dr. Julius Hagemann. It is also sometimes referred to as Side-looking Sonar or Side-imaging Sonar due to the fact that it only scans the areas to the side of the tow fish and not those directly below it. It has several frequency, range and resolution parameters as well as gain and display contrast values which can be modified according to the water conditions, the speed of the vessel and the aim of the scan; such that fast scans will use lower resolution, larger range areas, and possibly faster frequency signals to obtain the best possible image from a quick and broader glance at the seafloor surface. The opposite will hold for more detailed scans of the seafloor surface. The general principle behind the side scan is that it sends out regular acoustic (frequency) signals which will bounce back, in a stronger or weaker manner, and be recorded by the Sonar receptors. The data, containing strength, time elapsed and amplitude of the signal, will then be sent to the surface interface and interpreted by the console, which will produce a grey-scaled image of the seafloor surface as the Side Scan is towed along. The survey line is also saved and can then be converted to image files so that they can also be viewed on programs such as Google Earth, in a way similar to how images from the GPS are plotted to produce a constantly updated view of the world. The lab course was carried out from the 13th April to the 15th April off the coast of Helgoland, although data was only collected on April 14th. A trial run (line No. 0) was done on April 13th as practice and system check up for the next day. This survey line was actually run for a long time, which let me know that they should be stopped every so often and restarted to avoid huge data files. None-the-less, during that first run nothing much was observed, and it was not until the next day that some more interesting findings such as a shipwreck, sediment ripples, hills/mounds/big ripples or ridges on the seafloor (from my perspective, and upon further inspection of the images, they are more like big ripples than individual hills), different sediment types as well as some boulders and fish were seen. A second sunken object was spotted, although the console temporarily froze and not too much was recorded for the area. It did however appear to be some sort of object, although I am more inclined to say that it looks more like a depression or a dent in the seafloor surface, since a clear lighter colored rim is visible around a darker shaded middle area. Some very nice sediment ripples were also observed.

Limitations to the Side Scan are namely the speed of the vessel, the water conditions such as turbidity; sediment composition, since soft sediments will absorb the signals and limit the amount of signals, and therefore data, recorded; and depth of the Side Scan with regard to the depth of the seafloor; the closer to the seafloor the better the image resolution and data collection, however the

risk of the tow fish hitting an outcrop or the seafloor itself is too big to make it worthwhile, since the instrument would be lost. But not only the tow fish, the whole setup can give problems; as happened with us when the console froze and had to be rebooted. Data can also be lost if the tow fish passes over a cable or pipe that runs through the seafloor, in which case a horizontal line will cross the whole data and ruin the scan-lines in that latitude. None-the-less there are also many advantages to the Side Scan Sonar, namely- it's impressive accuracy for mapping the seabed, seafloor structures and outcrops, sediment types, and sunken objects. It is most useful when working in turbid waters, where visibility is very limited.

5.5 References

5.5.1 Text references

NOAA. Office of Coast Survey, "Side Scan Sonar." Learn About Hydrography. 2009. United States Office of Coast Survey. 26 May 2009. <http://www.nauticalcharts.noaa.gov/hydrography/side-scan-sonar/>.

NOAA. Coastal Services Center, "Side Scan Sonar." Benthic Habitat Mapping. 2009. United States Office of Coast Survey. 26 May 2009. <http://www.csc.noaa.gov/benthic-habitat-mapping/side-scan-sonar/>.

Starfish. The seabed is your playground. "WHAT IS SIDE SCAN SONAR?." Starfish. Seabed Imaging Systems. 2009. Trittech International Limited. 26 May 2009. <http://www.starfishsonar.com/technology/sidescan-sonar.html>.

Trittech International Ltd, "Trittech SeaKing Towfish Side Scan Sonar System. "Trittech Side Scan Sonar Systems". 2009. 26 May 2009. <http://www.tritech.co.uk/products/side-scan-sonar/>.

Woods Hole Oceanographic Institution, "Side-Scan Sonar Images." Voyage to Puna Ridge. 1998. Woods Hole Oceanographic Institution. 26 May 2009. <http://www.punaridge.org/doc/factoids/Default.html>.

5.5.2 Image references

Figures 1 and 2 were taken from Woods Hole Oceanography Institution Voyage to Puna Ridge.

Figure 3 was made by me.

Figure 4 was taken from Woods Hole Oceanography Institution Voyage to Puna Ridge, although I did some editing on it.

Figure 5 was taken from page 16 of issue 1 of the Trittech International Ltd SeaKing Side Scan Sonar System manual.

Figures 7-13 are screenshots taken from the Side Scan Console.

Survey line images were taken from the Challenger folder where all the data and files pertaining to the Heincke excursion are uploaded.

6 Marine Magnetism

by Milen Iliev and Kin Ovanesov

6.1 Aim

The aim of this experiment was to use a ship-towed SeaSpy magnetometer to create a magnetic field profile of the area directly south of the island of Helgoland, encompassing the waters between 7° and 8.2° E, along the 54th north parallel. Two separate lines were measured in the course of two days, each roughly parallel to 54° N, during the time of the day, when the geomagnetic field was relatively stable. Data was gathered at a measurement rate of 1 Hz, and was processed by having observatory values of the geomagnetic field subtracted from it. A plot for each line was created, and major anomalies were identified and discussed.

6.2 Theory

Magnetic Field

Magnetic fields are produced by electric currents, which can be macroscopic currents in wires, or microscopic currents associated with electrons in atomic orbits. The magnetic field \mathbf{B} is defined in terms of force on moving charge in the Lorentz force law. The interaction of magnetic field with charge leads to many practical applications. Magnetic field sources are essentially dipolar in nature, having a north and south magnetic pole. The SI unit for magnetic field is the Tesla, which can be seen from the magnetic part of the Lorentz force law $\mathbf{F}_{\text{magnetic}} = q\mathbf{v}\mathbf{B}$ to be composed of $\frac{\text{N}\cdot\text{s}}{\text{C}\cdot\text{m}}$. A smaller magnetic field unit is the Gauss (1 Tesla = 10,000 Gauss).

Both the electric field and magnetic field can be defined from the Lorentz force law:

$$\mathbf{F} = \underbrace{qe}_{\text{electrical force}} + \underbrace{q\mathbf{v} \times \mathbf{B}}_{\text{magnetic force}} \quad (6.1)$$

Magnetic Field Strength (**H**) The magnetic fields generated by currents and calculated from Ampere's Law or the Biot-Savart Law are characterized by the magnetic field **B** measured in Tesla. But when the generated fields pass through magnetic materials which themselves contribute internal magnetic fields, ambiguities can arise about what part of the field comes from the external currents and what comes from the material itself. It has been common practice to define another magnetic field quantity, usually called the "magnetic field strength" designated by **H**. It can be defined by the relationship

$$\mathbf{H} = \frac{\mathbf{B}_0}{\mu_0} = \frac{\mathbf{B}}{\mu_0} - \mathbf{M} \quad (6.2)$$

It unambiguously designates the driving magnetic influence from external currents in a material, independent of the material's magnetic response. The relationship for **B** can be written in the equivalent form

$$\mathbf{B} = \mu_0(\mathbf{H} + \mathbf{M})$$

H and **M** will have the same units, $\frac{A}{m}$. To further distinguish **B** from **H**, **B** is sometimes called the magnetic flux density or the magnetic induction. The quantity **M** in these relationships is called the magnetization of the material. [?]

Magnetic Properties of Solids

Materials may be classified by their response to externally applied magnetic fields as diamagnetic, paramagnetic, or ferromagnetic. These magnetic responses differ greatly in strength. Diamagnetism is a property of all materials and opposes applied magnetic fields, but is very weak. Paramagnetism, when present, is stronger than diamagnetism and produces magnetization in the direction of the applied field, and proportional to the applied field. Ferromagnetic effects are very large, producing magnetizations sometimes orders of magnitude greater than the applied field and as such are much larger than either diamagnetic or paramagnetic effects.

The magnetization of a material is expressed in terms of density of net magnetic dipole moments μ in the material. We define a vector quantity called the magnetization **M** by

$$\mathbf{M} = \frac{\mu_{total}}{V} \quad (6.3)$$

Another commonly used form for the relationship between **B** and **H** is

$$\mathbf{B} = \mu_0 \mathbf{H} \quad (6.4)$$

where

$$\mu = \mu_m = K_m \mu_0$$

μ_0 being the magnetic permeability of space and K_m the relative permeability of the material. If the material does not respond to the external magnetic field by producing any magnetization, then $K_m = 1$. Another commonly used magnetic quantity is the magnetic susceptibility which specifies how much the relative permeability differs from one.

Magnetic susceptibility $\chi_m = K_m - 1$

For paramagnetic and diamagnetic materials the relative permeability is very close to 1 and the magnetic susceptibility very close to zero. For ferromagnetic materials, these quantities may be very large.

The unit for the magnetic field strength H can be derived from its relationship to the magnetic field B , $B = \mu H$. Since the unit of magnetic permeability μ is $\frac{N}{A^2}$, and then the unit for the magnetic field strength is:

$$\frac{T}{\frac{N}{A^2}} = \frac{\frac{Nm}{Am}}{\frac{N}{A^2}} = \frac{A}{m}$$

An older unit for magnetic field strength is the oersted: $1A/m = 0.01257\text{oersted}$.
[?]

6.2.1 The Earth's Magnetic Field

When describing the magnetic field strength of the earth, it is more common to use units of nanoteslas (nT), where one nanotesla is 1 billionth of a tesla. The average strength of the Earth's magnetic field is about 50,000 nT.

Magnetic Equator - The location around the surface of the Earth where the Earth's magnetic field has an inclination of zero (the magnetic field vector F is horizontal). This location does not correspond to the Earth's rotational equator.

Magnetic Poles - The locations on the surface of the Earth where the Earth's magnetic field has an inclination of either plus or minus 90 degrees (the magnetic field vector F is vertical). These locations do not correspond to the Earth's north and south poles.

As observed on the surface of the earth, the magnetic field can be broken into three separate components.

Main Field

This is the largest component of the magnetic field and is believed to be caused by electrical currents in the Earth's fluid outer core (dynamo). For exploration

work, this field acts as the inducing magnetic field. Circulation in core changes with time: secular variations.

External Magnetic Field

This is a relatively small portion of the observed magnetic field that is generated from magnetic sources external to the earth. This field is believed to be produced by interactions of the Earth's ionosphere with the solar wind. Hence, temporal variations associated with the external magnetic field are correlated to solar activity. Changes with time: diurnal variations.

Crustal Field

This is the portion of the magnetic field associated with the magnetism of crustal rocks. This portion of the field contains both magnetism caused by induction from the Earth's main magnetic field and from remanent magnetization, which is the magnetic field element, that was 'locked' in the rock when it lithified or crystalized..

The magnetic field varies with time.

Secular Variations - These are long-term (changes in the field that occur over years) variations in the main magnetic field that are caused by fluid motion in the Earth's Outer Core. Because these variations occur slowly with respect to the time of completion of a typical exploration magnetic survey, these variations will not complicate data reduction efforts.

Diurnal Variations - These are variations in the magnetic field that occur over the course of a day and are related to variations in the Earth's external magnetic field. This variation can be on the order of 20 to 30 nT per day and should be accounted for when conducting exploration magnetic surveys.

Magnetic Storms - Occasionally, magnetic activity in the ionosphere will abruptly increase. The occurrence of such storms correlates with enhanced sunspot activity. The magnetic field observed during such times is highly irregular and unpredictable, having amplitudes as large as 1000 nT. Exploration magnetic surveys should not be conducted during magnetic storms.

Magnetics and Geology

The induced field relates to the existence of rocks of high or low magnetic susceptibility near the instrument. If measurements are taken near rocks of high magnetic susceptibility, magnetic field of higher strength will be measured. The strength of the field will decrease if the measurements will be taken at a greater distance from rocks of high magnetic susceptibility.

[?]

6.3 Instruments: The Magnetometer

The magnetometer which was used (SeaSPY) is a Total Field magnetometers, i.e. it measures only the magnitude of the magnetic field vector, independent of its direction with respect to the sensor. In comparison Vector magnetometers have the ability to measure the component of ambient field that is projected along one dimension in space. In order to calculate the total field, three separate vector magnetometer sensors must be oriented at right angles to each other, and their outputs geometrically added by a single processor. There are some practical limitations to how precisely and how rigidly the three sensors can be fixed together at exactly right angles. This is the reason, why the total-field precision of even the best flux-gate magnetometers is limited to an order of magnitude less than a SeaSPY magnetometer. Also the output of all vector-field sensors will experience drift with the time and with temperature. Vector magnetometers require periodic calibration with an accurate reference such as a proton-spin magnetometer. Proton-spin magnetometers never require calibration. These are the reasons, why total-field magnetometers are inherently superior to vector magnetometers when the task is detection of ferromagnetic anomalies within the Earth's magnetosphere.

A standard proton-spin magnetometer sensor begins with a small volume of proton-rich fluid such as methanol. Polarization of the protons in the fluid is caused through induction of a large temporary artificial magnetic field around the liquid. Once the proton population has been polarized, the proton spin axes are stimulated to precess around the ambient magnetic field vector. This process is known as deflection. The alternating magnetic field generated by proton precession may be detected by a coil, and its frequency measured by the magnetometric electronics. This frequency is directly proportional to the magnitude of the ambient field vector.

The difference between proton and Overhauser magnetometers is most apparent in the way that the proton populations are biased. The Overhauser effect is a phenomenon that uses electron-proton coupling to achieve proton polarization. SeaSPY Overhauser magnetometer sensors can produce clear and strong proton precession signals using only 1-2W of power. In contrast, standard proton sensors cannot produce signals that approach the same order of magnitude. SeaSPY's resolution is 0.001nT and it is highly sensitive and accurate (0.1nT) in comparison to the proton magnetometers. [?]

6.4 Data Collection

Data was collected in two runs, on two consecutive days. The towfish was towed by its cable from a small boat at a distance of around 70 m. The boat itself followed the Heincke at a variable distance of 80 to 120m, so that magnetic interference from the ship's hull is minimized. Figure ?? describes the physical setup of the equipment.

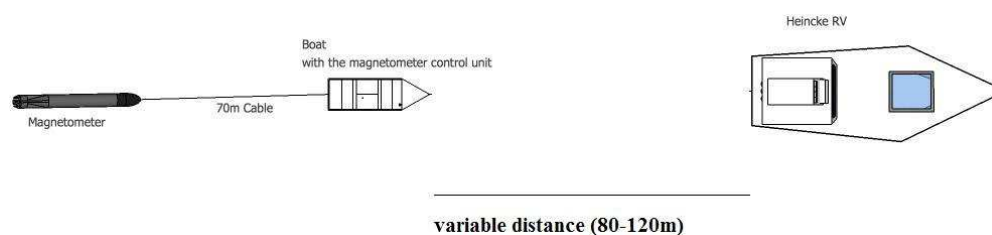


Figure 6.1: Physical setup of the magnetometer measurements.

The system for powering the magnetometer and recording the data was housed in a briefcase, which contained a DC battery power unit, an AC converter, a Toughbook laptop, and a GPS receiver. The towfish, the laptop and the GPS receiver all received their power from the converter. Data was passed from the GPS receiver and the towfish to the laptop. Figure ?? illustrates the setup of the system.

The properties of the lines are summarized in the tables below (Tables ?? and ??):

Line 1:				
Filename:Line_1.xls				
	Date	Time (UTC)	Latitude (°N)	Longitudde (°E)
Start	April 13, 2009	15:08:06	54.042347	7.782093
End	April 13, 2009	16:52:04	54.073143	8.115106

Table 6.1: Table, summarizing relevant data for Line 1.

Line 2:				
Filename:Line_2.xls				
	Date	Time (UTC)	Latitude (°N)	Longitudde (°E)
Start	April 14, 2009	09:47:20	54.13202	7.737297
End	April 14, 2009	10:57:58	54.13267	7.957056

Table 6.2: Table, summarizing relevant data for Line 2.

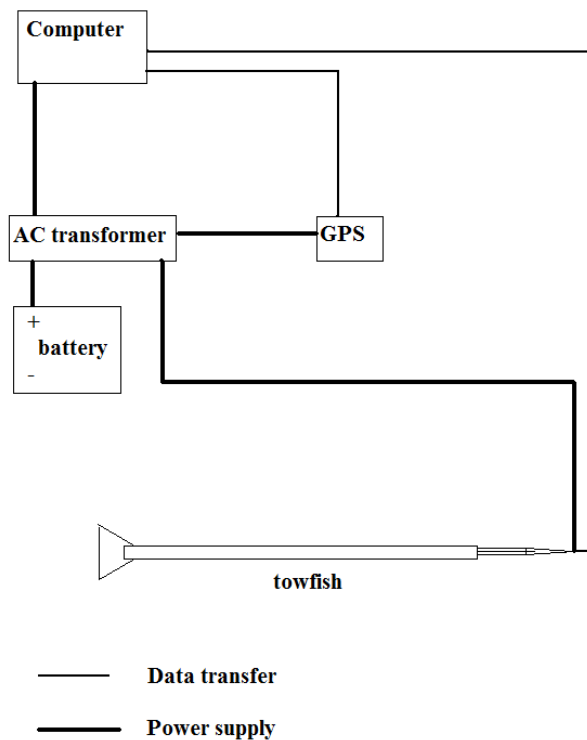


Figure 6.2: Electronical setup of the magnetometer system.

The location of the lines with respect to the island of Helgoland is shown on Figure ???. Line 1 passes through a military dumping site, and both lines pass through previously known ship wreckages.

Figure 6.3: Map of two magnetometer survey lines with respect to the island of Helgoland.

6.5 Data Processing

The data from the magnetometer was obtained at a rate of 1 Hz, while being towed at a speed of about 5 knots. This means that the resolution of the magnetometer profile is

$$resolution = \frac{5knots}{1Hz} \approx \frac{2.5m/s}{1Hz} = 2.5m$$

Data supplied by the magnetometer had a time stamp and a total magnetic field value. The system then obtained the proper longitude and latitude for each measurement from the GPS receiver system. Thus, the files have the format of a Spreadsheet with columns for date and time, longitude, latitude, and total magnetic field strength.

It should be noted, however, that by this stage the data has not been corrected for influences from the Earth magnetic field. In order to separate real local anomalies from global magnetic field changes, recordings for the International Geomagnetic Reference Field (IGRF) for the two days, during which the measurements were taken were obtained. The Braunschweig observatory Magnetsrode [?] was chosen because of the ease of access to its data, as well as for its geographical position - roughly on the same longitude and a few degrees of latitude to the south of the two lines.

To correct for the geomagnetic field influence, observatory values for the IGRF should be subtracted from the measured values. The remainder emphasizes the local anomalies and variations in the magnetic field, free from interference from the global magnetic field.

Ideally the observatory data would be taken every whole second, just as the towfish measurements are, which would then enable us to match the times from the towfish measurements with the times from the observatory and then subtract the result second by second. Unfortunately, the IGRF data measurements from Magnetsrode occasionally skip a second or two, during which seconds there are no measurements. This makes it impossible to match second-long measurements to each other, and an alternative method had to be found.

Fortunately, both lines were measured when the Earth magnetic field was in the stable phase of its diurnal cycle. (See Figures ?? and ??). Even though there is a slight slope in the curve, the difference between the end values is in the range of 1-5 nT, which is negligible. Furthermore, the magnetic observatory data shows no significant spikes, therefore assuring us that any spikes in our measurements are not due to the Earth magnetic field.

The approach used to process the data was quite simple. The average value of the observatory readings was taken for the period, when the magnetometer was active, and then this average value was subtracted from each measurement in the recorded data set. This produced a plot with the same slope, but different magnitude of the y-axis.

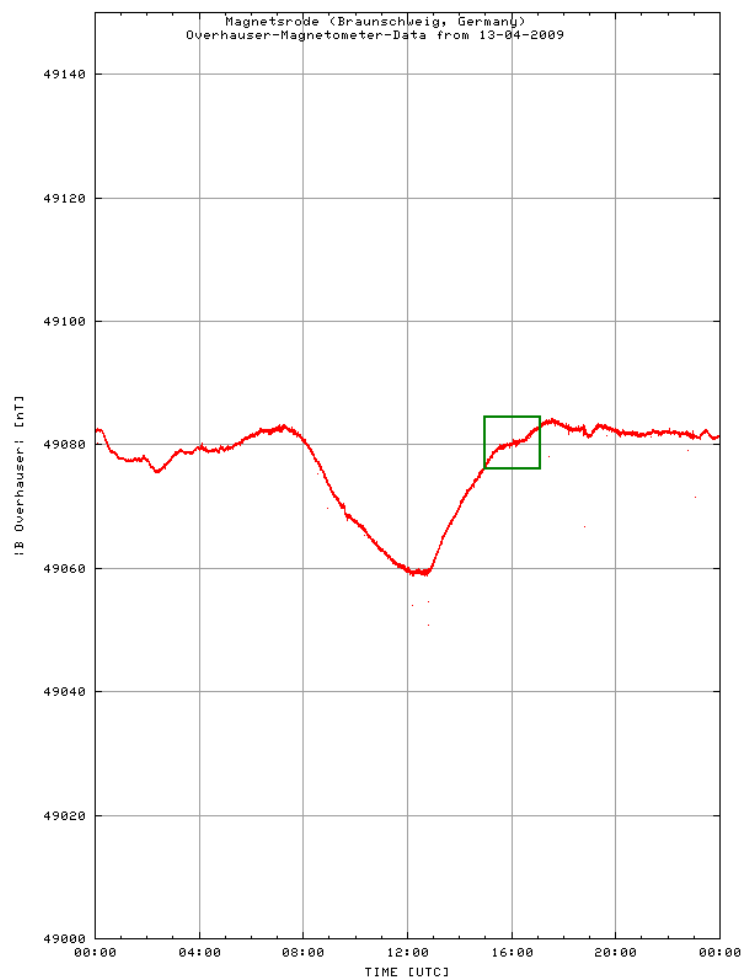


Figure 6.4: Braunschweig observatory data for first day, boxed is the time of measurement of Line 1. [?]

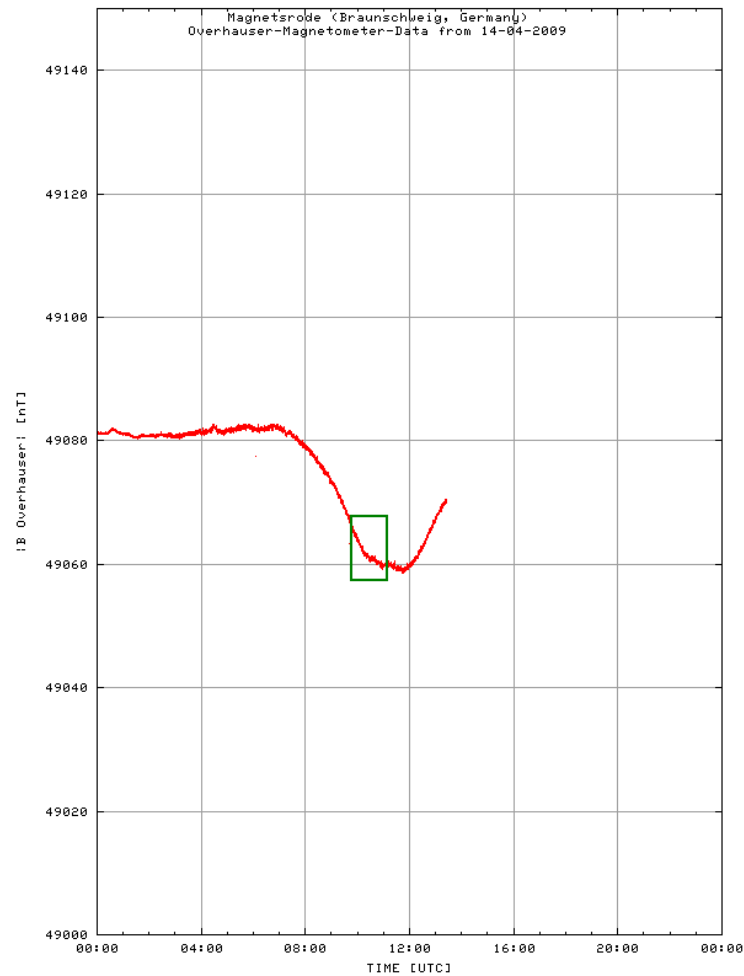


Figure 6.5: Braunschweig observatory data for seconds day, boxed is the time of measurement of Line 2., [?]

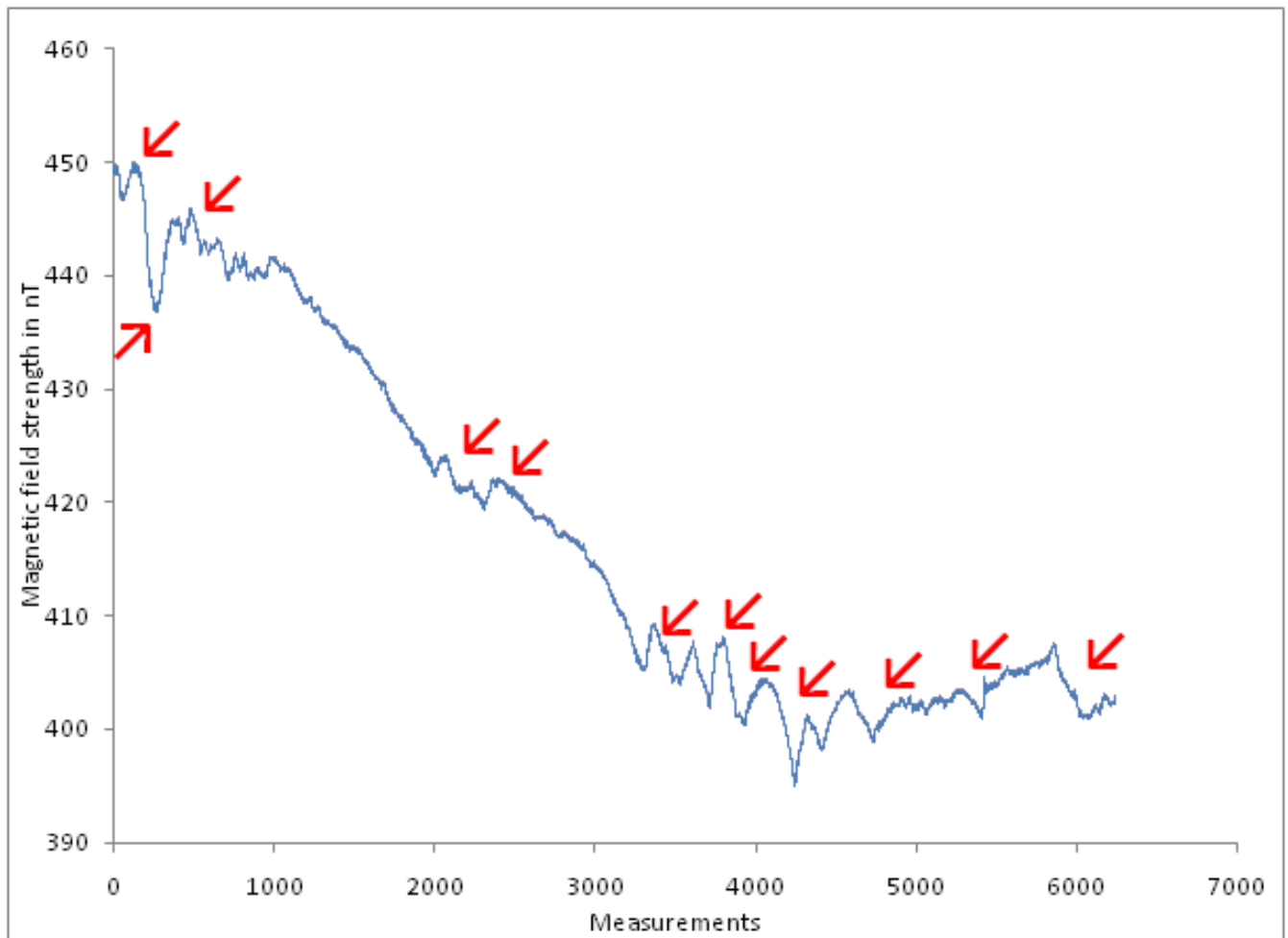


Figure 6.6: Empirical data with subtracted IGRF for Line 1. Red arrows indicated major anomalies.

6.6 Results and Analysis

Once the data was processed and the values from the Braunschweig observatory reading were subtracted, the data could be plotted. The plots are included below, with the x-axis showing the number of measurements, which also means the seconds elapsed since the start of the line, since all measurements are taken at a rate of 1 Hz. The y-axis is the strength of the local field minus the strength of the global magnetic field. Units are, as usual, nT. Anomalies are identified with a red arrow. The plots for the two lines are presented in Figures ?? and ?. It is also important to note that the number of measurements in Line 1 is larger, so the apparent slope is less steep than that of Line 2.

As can be clearly seen, there are numerous anomalies on the plots for both

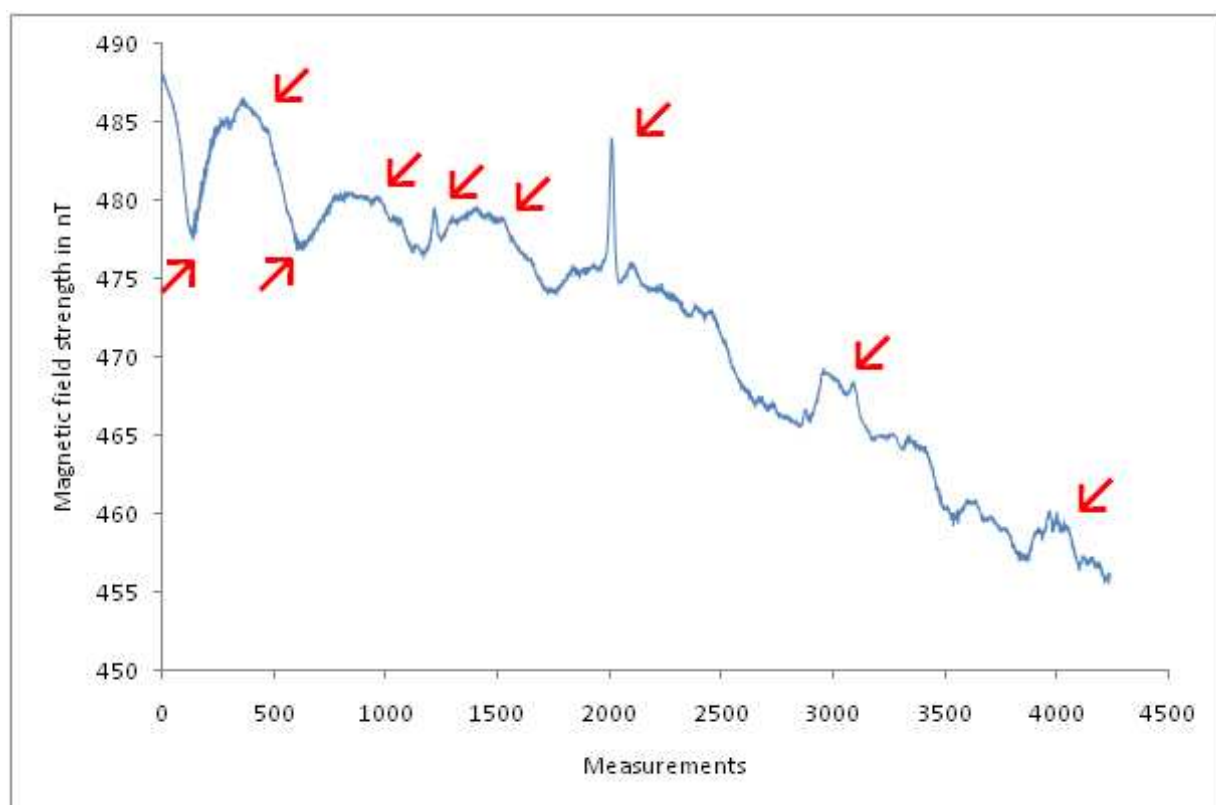


Figure 6.7: Empirical data with subtracted IGRF for Line 2. Red arrows indicated major anomalies.

lines. There are roughly two types of anomalies. One type is the sharp spike, that is most easily seen around measurement 2000 for Line 2. This usually results from a large metal object on the bottom, which in most cases is a shipwreck. This is actually the case for the 2000-measurement spike of Line 2 and some of the 3000-5000 measurement spikes of Line 1. The other type of anomaly is the gradual syncline or anticline that spans hundreds of measurements. This is most easily seen in the plot for Line 2. These anomalies can result from a number of things, such as the changing sand and clay content of the bottom sediment. Interestingly enough, going over the military munition dumping site did not produce any discernible anomaly in the plot. Perhaps a more sensitive magnetometer is needed, or the boat simply passed over few munitions in the zone.

It is also interesting to note that the magnetic field strength for the first line was larger on average by 30 nT. The lines passed over different areas, with a different type of bottom sediment within the Helgoländer Bucht. Line 1 passed over an area, which has a very high silt and clay content (above 50%). Line 2 passed over more sandy sediment with clay content between 5 and 20 %. [?]

Both Lines also passed over a fault line, but the fault anomaly could not be identified.

6.7 Discussion and Conclusions

There are several directions for further analysis of the data. One would be to try to find the anomalies that correspond to passing over a fault, and then compare the magnetometer profile with known maps of the region. Another direction of further analysis will be to obtain data from an observatory that takes measurement every second, without missing any. In this way, the IGRF can be subtracted on a second by second basis and thus arrive at a more accurate plot, since the current plots have an error of about 1 or 2 nT. This, of course, would not be a big improvement, but is a procedural improvement that can make a difference in other cases, where more sensitive measurements are required. If the slope is to be measured, this is important. Sources of error currently include the presence of the large metal body of the boat. Even though it is always stayed at least 150m away from the towfish, it produces an effect on the measurements. Fortunately, this effect is constant and does not affect the presence of magnetic anomalies. A slower speed of the boat would give better resolution, however the current resolution is good enough for most uses. The only thing it would have trouble detecting would be unexploded ordnance on the bottom of the sea, but in general the SeaSPY magnetometer is not meant to do that, since it is a surface-towed magnetometer. If smaller objects and

higher sensitivity is needed, a near-bottom should be used, if available. Other products by Marine Magnetics are advertised for the search of small metal objects, like SeaQuest. In general it can be concluded that the methods used for creating these two magnetometry profiles were scientifically sound, without introducing major flaws into the data set. Directions for improvement are to reanalyze the data more carefully, but as a whole, the profiling was successful - major anomalies were identified and correlated to the plot, for example, ship wrecks and differing sediment content. Because of its high precision, the data set still holds potential for deeper analysis. Also, the area around Helgoland is interesting from a geological and oceanographical point of view, and as of now, few magnetic profiles have been created. Further magnetic exploration could yield new and valuable information about the region.

Bibliography

- [Earth's Magnetic Field] <http://hyperphysics.phy-astr.gsu.edu/hbase/magnetic/ma>
(*Information on Earth's Magnetic Field*)
- [MarineMagnetics Website] <http://marinemagnetics.com/> (*Information on and specifications of the MarineMagnetics Explorer magnetometer*)
- [SeaSPY Tech Guide] http://www.marinemagnetics.com/pdf/SeaSPY_Tech_Guide.pdf
(*Information on Proton-Spin magnetometers and the Overhauser Effect*)
- [Magnetstrobe Datenarchiv] <http://www.igep.tu-bs.de/institut/einrichtungen/ma>
(*Magentsrode Datenarchiv*)
- [HyperPhysics] <http://hyperphysics.phy-astr.gsu.edu/hbase/emcon.html#emcon>
(*perPhysics: Electricity and Magnetism (2005)*)
- [Unnithan, V.] <http://www.faculty.jacobs-university.de/vunnithan/courses/sp>
(*nithan, V., Lectures Magnetism [PowerPoint slides]*)
- [Helgoland Sediment Map] (*Figge, K. Nordsee Sedimentverteilung in der Deutschen Bucht.*)

7 Echosounder

by Ishan Basyal

7.1 Introduction

An echo sounder is a device that sends sound waves to the bottom of the ocean floor and then, processes the echo received to build a structure of the target area. The research ship Heincke had two echo sounders. One was the Simrad K60 and the other one was the fisheries echo sounder.

Echo sounders are similar to SONAR in a sense that both use sound waves to produce an image of the seafloor topography and of other miscellaneous objects such as boulders, shipwrecks, fish, sediment ripples and so on. To get a better picture of the sea-floor, the vessel containing the echo-sounder should be moving very slowly as the signal received is stronger thus leading to a higher resolution. An echo-sounder is pretty effective in scanning the benthic zone as well as for locating fish populations as it can scan a large area in a few milliseconds of real time.

One of the interesting aspects about echo-sounder is that it has other purposes apart from research uses, in areas like fishing, looking for archaeological sites, sunken ships and so on.

7.2 Instruments on Board

The Heincke research vessel is equipped with one navigation echo sounder, two fisheries echo sounders, a net monitoring system and a sediment echo sounder. However, for our purposes two instruments on board were used: the side scan echo sounder and the built navigation echo sounder. The side scan echo-sounder was towed behind the ship and the navigation echo sounder was inbuilt to the ship. The side scan echo-sounder is used to locate the fish populations and is used mainly for fishing purposes.

7.3 Data collection

In the Heincke, the two echo-sounders were already connected and only the interface had to be used. The echo-sounders could be turned on and off from the interface itself, however they were running when the ships system were on. Therefore, there was no special way to turn them on and use them apart from running the interface to get the desired data. The interface has an internal processing of the data received to useful data and the profile of the data achieved was in a 2D plane, however the main screen could be divided into four parts that record the data at various frequencies. If the exact depth and the topology of an area isn't known in advance, it's better to use a range of frequencies, as high frequencies are good in mapping shallow areas whereas, low frequencies are good in mapping deep areas.

The data collected is presented in the Appendix section as it's too long to be presented here. ??

7.4 Visualization

An echo-sounder consists of an emitter and a recorder which is connected to an interface, that interprets the data to give a 2D image of the ocean floor. An echo-sounder transmits sound signals at both low and high frequencies, as different frequencies have different resolutions and a different image of the ocean floor can be obtained.

The signal travels through water until it strikes a hard object that can be anything from a fish, ship wreck or the ocean floor. After striking any object the signal is reflected back, this reflected signal is then picked up by the receiver in the echo-sounder and used to produce an image of the ocean bottom. Some part of the transmitted wave also penetrates the ground and the same image is relayed thus giving rise to multiples that occur at exactly the same distance as the depth between the ship and the first reflection. Multiples are the result of subsequent reflections of the initial energy.

In general the console uses the data acquired to produce a continuous image of the ocean floor and contrasting colors are used to show the varying intensities of the reflected wave. The effect of contrasts in analyzing the signals will be explained below with the pictures. The stronger signals occur when the wave strikes really hard solid objects and the signal is poor when the sediment is rather loose i.e. mud or sand slopes.

An echo-sounder has two consoles to acquire data. One console is just for the

imaging part whereas the other one is used to get the depth measurements of the sea-floor. The depth measurement is needed as to vary and adjust the emitting frequencies accordingly. As mentioned above, shallower depths require high frequency to get a better map whereas, deep waters are better imaged in low frequency.

The first console had an option of selecting the echo-sounders and managing the setting for it, as there were two echo-sounders on board, initially the Simrad— was taken and then the boats echo sounder was selected. The console also had an option to adjust which measurements to take and in which system e.g. metric or FPS or any other. In our case the SI units were taken to comply with the European standards. Then, the starting and end time were entered in UTC, and when the program (console) was run, the depth measurements for the given time interval was automatically saved in a file.

The second console was for controlling the frequency of the echo-sounder and also for imaging. The second console had a start/pause button and it was synchronized with the first console. The console could be manipulated to get the different frequencies from the echo-sounder and in our case it was manipulated to give four frequencies. The images from the four different frequencies were made to appear together on the screen. When the processing is started in the console, the information about the water environment, the sound speed, the total number of targets taken into account and all can be read in the right hand side of the output image. This will be illustrated in the following sections.

7.5 Results and Analysis

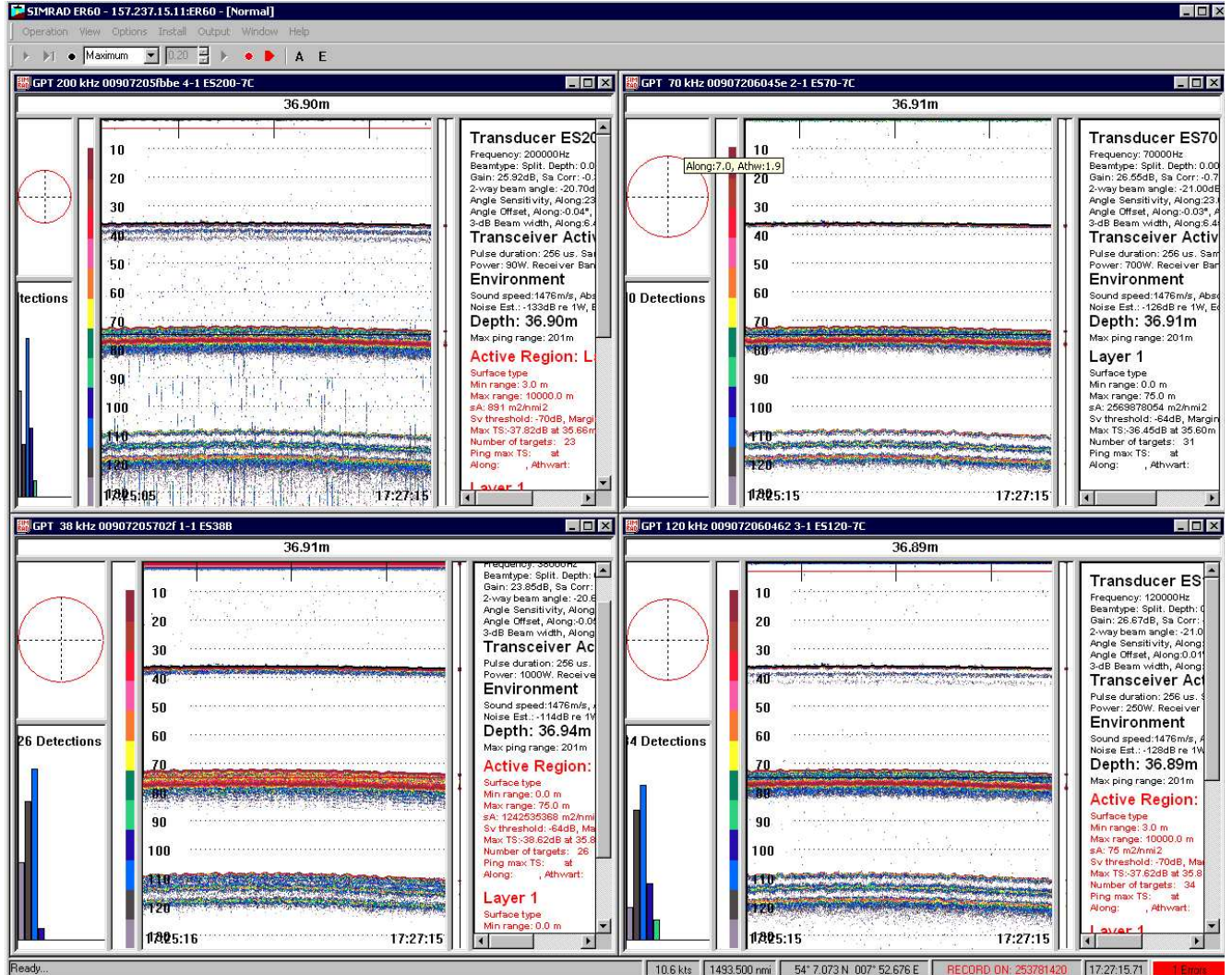


Figure 7.1: A normal over-view of the visualizing console

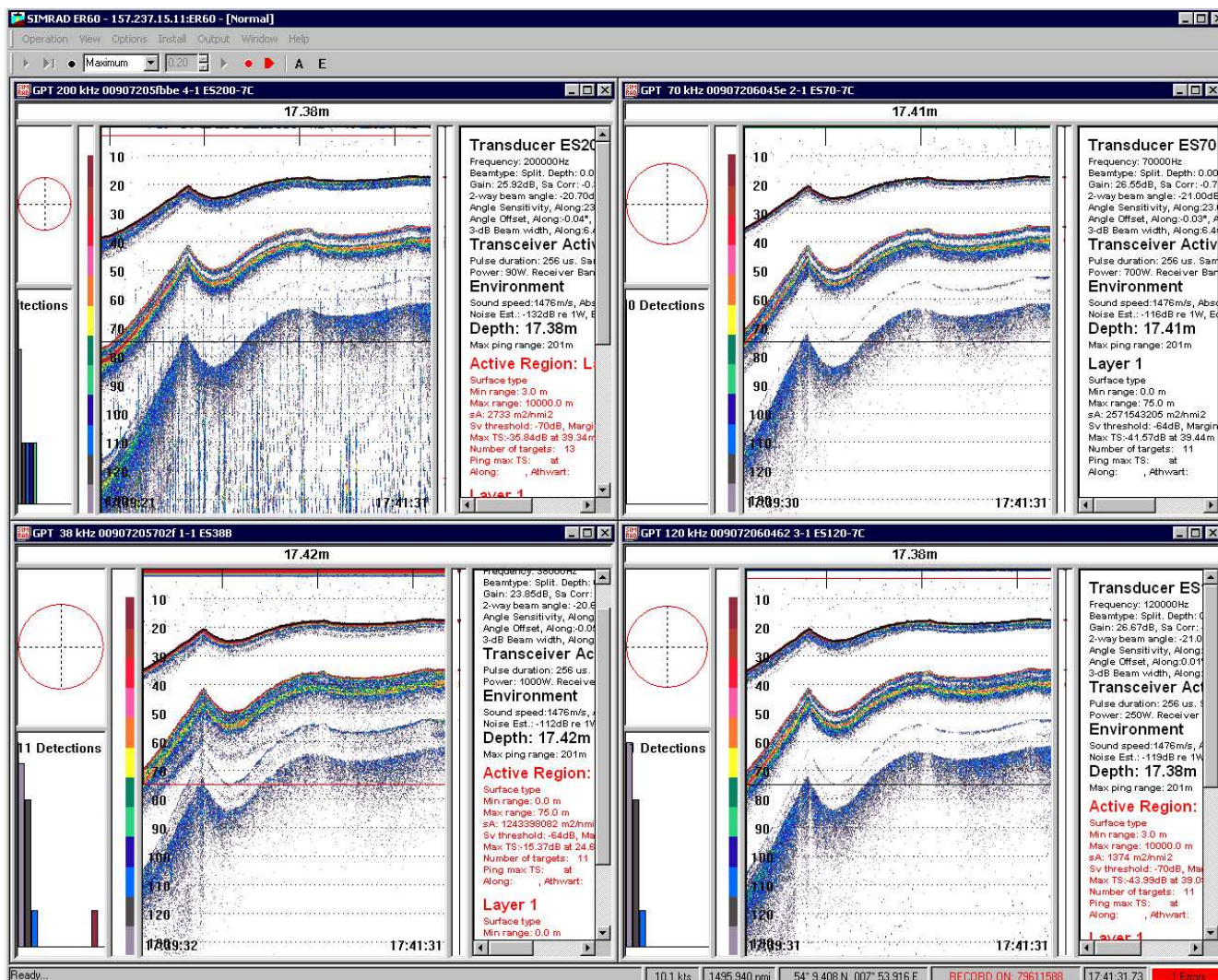


Figure 7.2: An image of the ocean floor from the first day, with some topographical change in the depth of the sea bed as the Heincke was nearing Helgoland

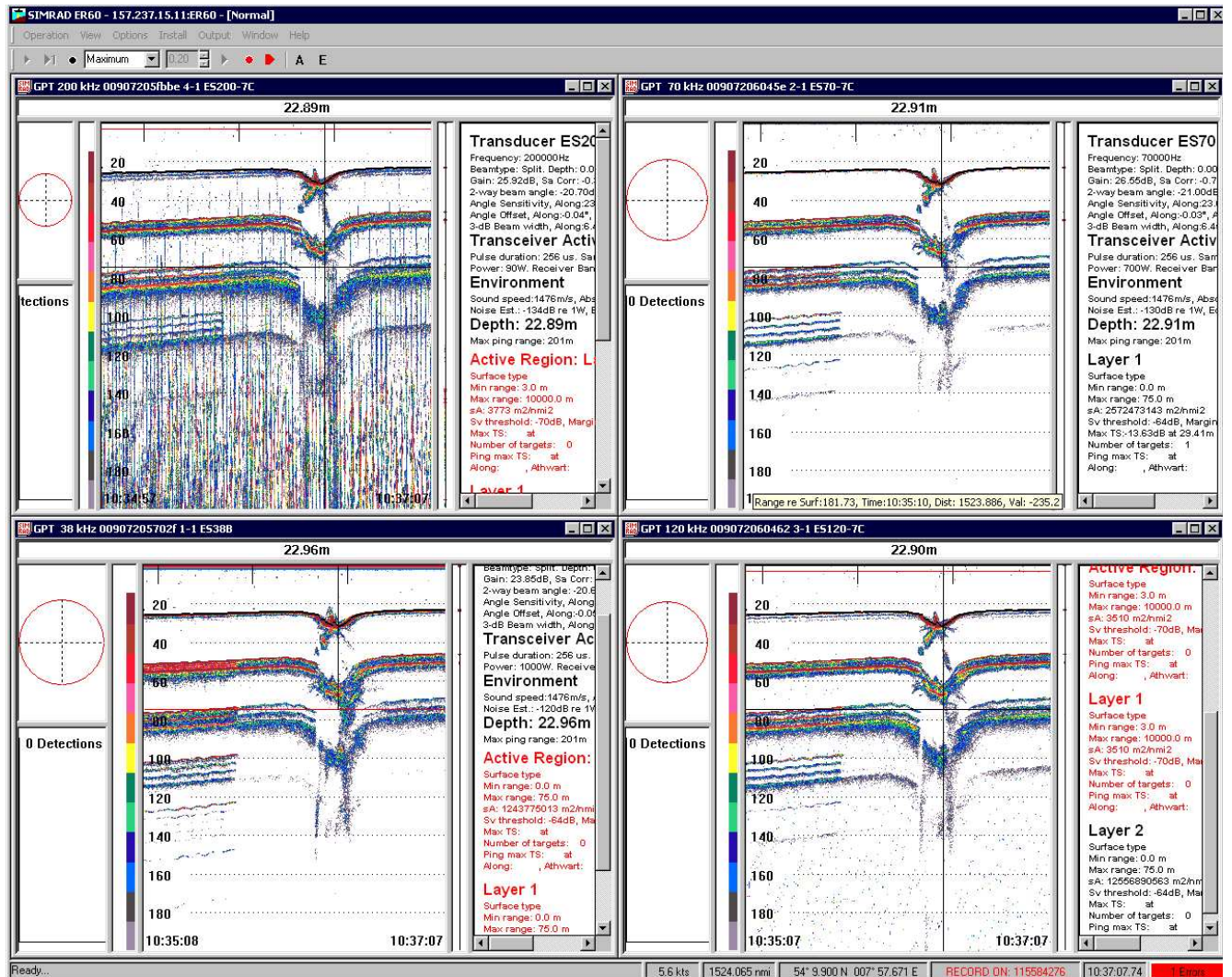


Figure 7.3: An image of the ocean floor from the second day, with some protruding structure on the bottom, which was later determined to be a ship wreck after the analysis from sonar and multibeam readings.

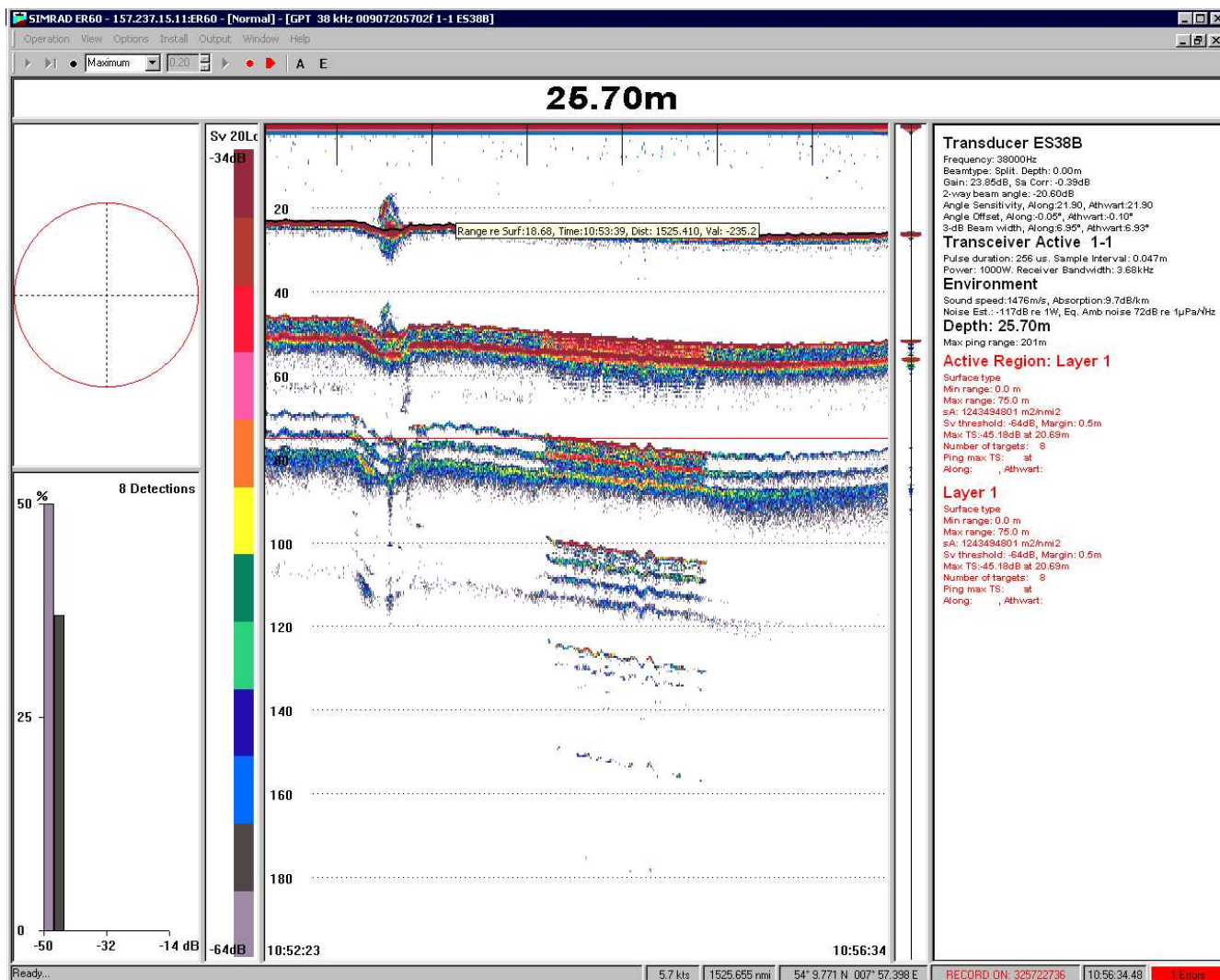


Figure 7.4: The same image as above but after a second visit.

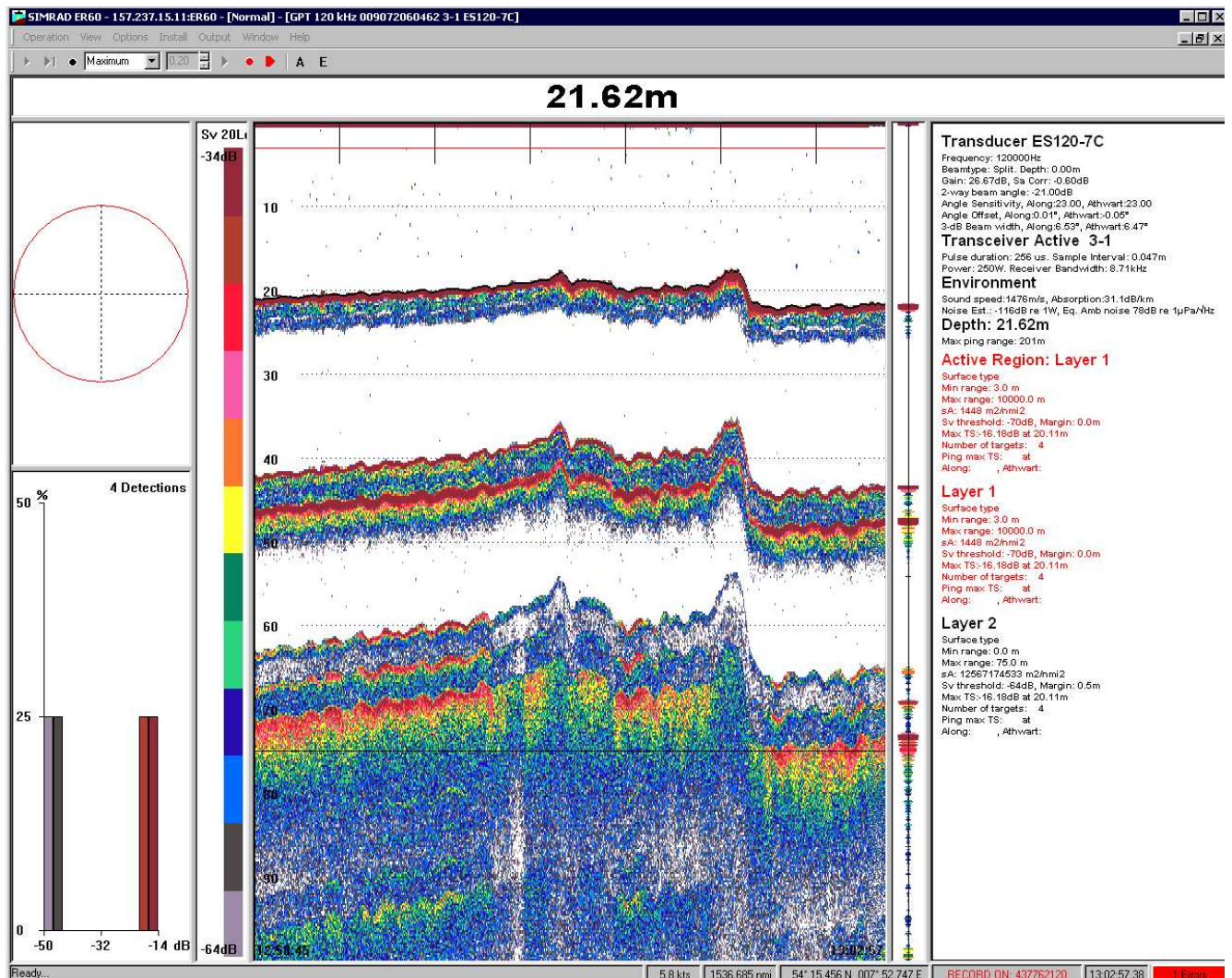


Figure 7.5: An image of the seabed showing the small underwater hillocks.

7.6 Discussion and Conclusion

The data obtained were very good as a range of frequencies were used to map the ocean floor. The higher frequencies have lower penetration power and are used to map shallower areas. Whereas, the lower frequencies are used to map the deeper areas. As, in our case a whole array of frequencies, namely 38 KHz, 70 KHz, 120 KHz and 200 KHz were used and then, the best diagram regarding the different areas were taken. So, in our case as the area was very shallow, the average depth was around 20 meters, so the best image were obtained from the highest frequency i.e. 200 KHz.

Then, the various structures were observed on the ocean floor. After analyzing the structures and comparing the results from the multibeam, sonar, and other sources, few ship wrecks were found. The ship wrecks make the same sort of depression as drop stones and can hence be identified, but some of the structures could be some dropstones as well.

If a seismic energy is reflected more than once, then it's known as a multiple. The interface depth and separation determine the additional reflections that are time dependent. The time lag depends upon the depth of the water i.e. it's shorter for shallow water and long time lags for deeper waters. The sea bottom multiples as in our case, can be interpreted as deeper reflections, that travel at lower velocities compared to a true reflection from that depth. And, as can be seen from the images provided above, it can be seen that the multiples as equal intervals, thus can be easily recognized.

8 General Discussion, Synthesis and Conclusions

by Jelle Bijma & Vikram Unnithan

9 Future Work and Collaborations

by Jelle Bijma & Vikram Unnithan

10 References

Example Bibliography

Bibliography

- [ref1] <http://hyperphysics.phy-astr.gsu.edu/hbase/magnetic/magearth.html>
(*Information on Earth's Magnetic Field*)
- [ref2] <http://marinemagnetics.com/> (*Information on and specifications of the MarineMagnetics Explorer magnetometer*)
- [ref3] http://www.marinemagnetics.com/pdf/SeaSPY_Tech_Guide.pdf (*Information on Proton-Spin magnetometers and the Overhauser Effect*)